Direct Infusion Lipidomics:
Profiling the Lipidome of a
Composite Tailings Reclamation Site

Direct Infusion Lipidomics:

Profiling the Lipidome of a

Composite Tailings Reclamation Site

By

Paul Allen Hodgson

B.Sc. (McMaster University, Hamilton) 2011

A Thesis

Submitted to the School of Graduate Studies

In Partial Fulfillment of the Requirements

For the Degree of

Master of Science

Chemistry

McMaster University

MASTER OF SCIENCE (Chemistry)

McMaster University

Hamilton, Ontario

TITLE:	Direct Infusion Lipidomics: Profiling the Lipidome of a Composite Tailings Reclamation Site
AUTHOR:	Paul Allen Hodgson, B.Sc. (McMaster University, Hamilton)
SUPERVISOR:	Professor Brian McCarry
NUMBER OF PAGES:	xi, 87

Abstract

The comprehensive analysis of intact lipids (called lipidomics) can provide information about the presence of microbial communities in an ecosystem and assist in understanding the biogeochemistry in that system. In previous work we had developed a method to determine the profiles of eight phospholipid classes in a soil microorganism by direct-infusion electrospray mass spectroscopy using tandem mass spectrometry. The work done in this study encompasses first the optimization of previous methodology for use with water and sediment samples containing low concentration of phospholipids and large amounts of organic contaminants and secondly the application of this method to the analysis of phospholipids within composite tailings and recycled process water using a triple quadrupole mass spectrometer to determine the intact lipids in the bacterial community. The results are presented illustrating the phosphatidylcholine (PC) and phosphatidylethanolamine (PE) lipids present in composite tailing samples and recycled process water.

This thesis begins with the optimization of a direct infusion mass spectrometry method, which allowed the analysis of intact phospholipids within both water and sediment samples. This method allows for high through-put analysis using both the separation afforded by neutral loss and precursor ion scanning modes and a database containing all possible adduct masses to identify and quantify unknown phospholipids.

This method was then applied to water and sediment samples obtained from the Syncrude Sandhill Fen composite tailings site. This analysis discovered multiple differences within the water samples attributed to changes both in well temperature and the ongoing reclamation projects resulting in the change in phospholipid profiles. This thesis also outlines the short-

comings of the direct infusion lipidomics method when used for the analysis of complex samples such as composite tailings sediment samples.

In summary, this thesis has demonstrated that direct infusion lipidomics can be successfully applied to the analysis of water samples and yield statistically significant differences within the microbial lipidome.

Acknowledgements

Dr. McCarry, words cannot express how thankful I am to have had the opportunity to work with you over the course of my thesis. I feel blessed to have known you and you truly were an inspiration. You will be greatly missed.

To my friends and fellow students of the McCarry group, Sujan Fernando, Roger Luckham, Fan Fei, David Bowman, Vi Dang and Ken Chalcraft I would like to thank you not only for your input and advice other the past two years but also for how enjoyable you all made it. It was a pleasure to come into work each day. A special thanks to Ken Chalcraft for guiding me in writing my thesis and in helping during the editing process. Next I would like to thank our collaborators Dr. Greg Slater and Dr. Lesley Warren as well as their research groups. It was a pleasure to work on the Syncrude project with all of you. I want to also like to thank the staff of the Mass Spec facility, mainly Dr. Kirk Green for all the training and troubleshooting that went into this project.

Finally, I will never be able to express enough thanks and gratitude to my parents Peter and Laura Hodgson, you have truly been an inspiration and wonderful role models for me on my journey. And to my fiancée Sabrina Van Gyzen, without your love and support none of this would have been possible. Thank you for being so amazing (and patient).

Table of Contents

Abstract ii

Acknowledgements iv

Table of Contents v

List of Figures vii

List of Abbreviations x

1. Chapter 1: Introduction 1

1.1 A Brief History of the Canadian Oil Sands 1

1.2 Alberta Oil Sands Extraction Techniques 3

1.3 Introduction to Lipidomics 6

1.4 Structure and Naming of Lipids 9

1.5 Current Analytical Techniques for Phospholipid Analysis 12

1.6 Introductory to Mass Spectrometry 14

1.7 Electrospray Ionization 16

1.8 Introduction to Mass Analyzers used in phospholipid analysis 20

1.9 Multi-dimensional Mass Spectrometry by QQQ-MS 21

2. Chapter 2: Methods and Materials 25

2.1 Equipment and Chemicals 25

2.1.1 Other Instruments 25

2.2 MS Parameters 26

2.3 Data Processing and Extraction 26

2.4 Statistical Analyses 27

2.5 Water and Sediment Sample Collection, Preparation, and Extraction 27

3. Chapter 3: Direct Infusion Method Development 34

3.1 Optimization of Current Mass Spectrometry Method 34

3.2 Phospholipid Theoretical Exact Mass Database 38

3.3 Phospholipid Fragmentation database 39

4. Chapter 4: Results 42

4.1 Calibration Standards 42

4.2 Syncrude Composite Tailings Well Water Samples 46

4.3 Syncrude Composite Tailings Well Sediment Samples 66

5. Chapter 5: Discussion 68

5.1 Calibration Standards 68

5.2 Syncrude Composite Tailings Well Water Samples and Multivariate Analysis 71

5.3 Syncrude Composite Tailings Well Sediment Samples 76

6. Chapter 6: Conclusion and Future Direction 78

6.1 Conclusions 78

6.2 Future Directions 80

7. Appendix 1: List of Chemical Standards Used 85

List of Figures

Chapter 1

Figure 1.1 - Map of Alberta and Saskatchewan depicting the location of known oil sands deposits. (Reproduced from CAPP 2013 Annual Report)[49] 3
Figure 1.2 - Number of publications containing the keyword "lipidomics" as of December 5th, 2013 as per Web of Science 8
Figure 1.3 - Structure and variations of common lipid classes 10
Figure 1.4 - Detailed Structure of phospholipids 11
Figure 1.5 – 1-palmitoyl-2-oleoyl-sn-glycero-3-phosphocholine, known as PC 34:1 or PC 16:1/18:0 11
Figure 1.6 Comparison of three of the most commonly used ionization methods for lipidomics analysis[19] 14
Figure 1.7 - Ion evaporation model of electrospray ionization 17
Figure 1.8 - Free-jet/Coulombic fission model of electrospray ionization 18
Figure 1.9 Commonly used mass analyzers and their characteristics (adapted from DASS; "Principles and Practice of Biological Mass Spectrometry" Wiley Interscience New York 2001). (Q-Tof=quadropole-time-of-flight; FT-ICR=fourier transform - ion cyclotron resonance) 20
Figure 1.10b - Visual representation of precursor ion scan mode 23

Chapter 2

Figure 2.1 - Mass Spectrometer parameters used for the acquisition of mass spectrum of phospholipids 26
Figure 2.2 - Top: Map of Alberta depicting the location of the Syncrude mining site 29
Figure 2.3 – Locations of the sampling wells within the Sandhill Fen 30
Figure 2.4 - Sandhill Fen cross section 30
Figure 2.5 - Depths and final layer locations of the sampling wells in the Sandhill fen 30

Chapter 3

Figure 3.1 - Intensity of lipid standards versus resolution, where resolution was calculated using the PC 14:0/16:0 internal standard (m/z 712) 35
Figure 3.2 - Peak intensities of phospholipid standards versus the capillary voltage (kV) 36
Figure 3.3 - Peak intensities of phospholipid standards versus LiCl concentration 37
Figure 3.4 - Phospholipid lookup interface for positive mode lipids (PE and PC) 39
Figure 3.5 - Product ion scan of m/z 712, PC 16:0/14:0, highlighting the loss of the tail units... 40
Figure 3.6 - Tail loss lookup interface for determining possible combinations of tail units on a given phospholipid. In this example PC 16:0/14:0 from Figure 3.4 is shown..... 41

Chapter 4

Figure 4.1 - Relative response of PE standards compared to the internal standard PE 14:0 44
Figure 4.2 - Relative response of PE standards compared to the internal standard PC 16:0/14:0 45
Figure 4.3 - Phosphatidylcholine (PC) and phosphatidylethanolamine (PE) profiles in the Sump Vault July 2011 47
Figure 4.4 - Phosphatidylcholine (PC) and phosphatidylethanolamine (PE) profiles in the Sump Vault July 2011 with an +42m/z offset applied to the PE spectrum..... 48
Figure 4.5 - Loadings plot for the PCA plot of all well samples 51
Figure 4.6 - Principal Component Analysis of all well samples over all time points..... 51
Figure 4.7 - S-Plot for the OPLS-DA plot of Well 6A over four time points 53
Figure 4.8 - OPLS-DA plot of Well 6a over four time points 53
Figure 4.9 - S-Plot for the OPLS-DA plot of the Sump Vault samples..... 55
Figure 4.10 - OPLS-DA plot of the Sump Vault over an 11 month span showing seasonal differentiation..... 55
Figure 4.11 - S-Plot for the OPLS-DA plot of the Well 8c samples 57
Figure 4.12 - OPLS-DA plot of Well 8c showing 3 time points over a one year period 57
Figure 4.13 - S-Plot for the OPLS-DA plot of the July 2011 samples 59
Figure 4.14 - OPLS-DA plot for all well samples from July 2011..... 59

Figure 4.15 - S-Plot for the OPLS-DA plot of the May 2012 samples..... 61
Figure 4.16 - OPLS-DA plot showing a moderate trend between four of the wells during the May 2012 sampling period..... 61
Figure 4.17 - S-Plot for the OPLS-DA plot of all the water samples..... 63
Figure 4.18 - OPLS-DA plot of all samples showing no trends..... 63
Figure 4.20 - OPLS-DA plot showing a moderate trend between summer months versus the rest of the year..... 65
Figure 4.19 - S-Plot for the OPLS-DA plot showing the summer months vs the rest of the samples..... 65
Figure 4.21 - Mass spectrum of the Well 6a soil sample July 2011 showing large amount of ion suppression and lack of recovery..... 67

Chapter 5

Figure 5.1 - Internal standard consistency across multiple injections..... 68

List of Abbreviations

APCI: atmospheric pressure chemical ionization

CID: collision induced dissociation

EI: electron ionization (electron impact)

ESI: electrospray Ionization

FA: fatty acid

FAMEs: fatty acid methyl esters

FT-ICR: Fourier transform ion cyclotron resonance mass analyzer

GC/MS: gas chromatography coupled to mass spectrometry

HPLC: high performance liquid chromatography

LOD: limit of detection

LOQ: limit of quantification

m/z: mass to charge ratio

MALDI: matrix assisted laser desorption ionization

MRM: multiple reaction monitoring

MS: mass spectrometry

MS/MS: tandem mass spectrometry

NL: neutral loss

OPLS-DA: orthogonal projections to latent structures - discriminant analysis

PA: phosphatidic acid

PC: phosphatidylcholine

PCA: principal component analysis

PE: phosphatidylethanolamine

PG: phosphatidylglycerol

PI: phosphatidylinositol

PS: phosphatidylserine

QQQ: triple quadrupole mass analyzer

Q-TOF: quadrupole time-of-flight mass analyzer

SAGD: steam assisted gravity drainage

TOF: time-of-flight mass analyzer

Chapter 1: Introduction

1.1 A Brief History of the Canadian Oil Sands

The Alberta oil sands deposit was originally documented nearly 200 years ago when James Knight, a fur trader in the area wrote about a gummy tar like substance on the banks of the Athabasca river[1]. This substance was the bitumen that was so abundant in the area; bitumen is a highly viscous, stinky, petroleum based product[2]. As research into the extraction of bitumen from the sand progressed Dr. Karl Clark of the Alberta Research Council pioneered a hot water based extraction method in the 1920s that allowed bitumen to be separated efficiently from the sand[3]. It wasn't until the 1940s however, that the oil sands were used for the production of diesel fuel. The initial interest into the production of diesel fuels was sparked in part, due to the large demand caused by the Second World War. During this time, the Canadian government took control and expanded the production facilities of the major company operating in the Alberta Oil Sands, Abasand Oil, in order to secure fuel required for the war effort[4]. The realization that these reserves could be utilized in a similar manner to the traditional oil wells fueled further research into the bitumen refining process. In 1962 the Canadian government put forward an initial set of regulations regarding the development of the Alberta oil sands and large scale production facilities were approved. Syncrude, a major company currently in operation in the oil sands and major support of this thesis, was initially founded in 1964 but did not receive approval for their site until 1969. Construction began in 1973 and the first barrels of oil were shipped in 1978. Production by Syncrude Canada has increased tremendously over the years and in 2011 they produced 105.3 million barrels of crude oil[5].

As of December 2012 Canada is home to the third largest crude oil reserve in the world, containing an estimated 173-175 billion barrels of crude oil, behind only Venezuela and Saudi Arabia which have estimated reserves of 297 billion and 265 billion barrels of crude oil respectively. The Alberta oil sands, shown on a map of Alberta and Saskatchewan in Figure 1.1, constitute 97% of the entire Canadian oil reserve containing 168 of Canada's 173 billion barrels of oil[6]. These reserve only account for oil that can be economically extracted using current technology. The current rate of production in the Alberta oil sands is estimated to be 1.3 million barrels of oil per day.

Figure 1.1 - Map of Alberta and Saskatchewan depicting the location of known oil sands deposits. (Reproduced from CAPP 2013 Annual Report)[50]

1.2 Alberta Oil Sands Extraction Techniques

There has been a tremendous amount of research into extraction techniques for the separation of bitumen from the sand and currently numerous methods exist allowing companies to advantage of the vast reserves of bitumen found in the Canadian oil sands. The oldest and still one of the most widely used methods involves the open pit mining of the bitumen ore. The ore is then crushed to reduce the size, hot water is added (50-80° C) to form a slurry that is easier for the machinery to manipulate. It is then put into a separation vessel where bitumen froth forms and floats to the surface where it can be skimmed off and separated from the rest of the mixture. This froth will typically contain roughly 60% bitumen, 30% water and the remaining 10% sand and other solids[7]. This froth is further refined removing the 40% of water and solid material. Overall, this method is capable of extracting between 60-90% of the bitumen found within the sand. The remaining bitumen along with the sand and water are then put into large tailings ponds, typically these ponds are created in an exhausted open pit mine. The solid material is allowed to settle out of solution and the remaining mixture can be removed. This remaining mixture of water and fine particulate matter is called the fluid fine tailings; this mixture is removed from the tailings pond and treated with a flocculating agent, such as gypsum. This helps to improve the settling process of the fine material by having large flocculating agents aggregating with the fine material to settle out of solution. This mixture of fluid fine tailings and gypsum is called the composite tailings, these are further dewatered and put back into exhausted mine pits where they continue to be dewatered. Syncrude has begun exploring the effects of covering the composite tailings with a sand cap with the goal of returning the land to its original state. The water that is removed during the dewatering steps can be reused in the extraction process[8].

The second method most common method is called steam-assisted gravity drainage (SAGD). The SAGD method, first developed by Dr. Roger M. Butler in the 1970s[9], is a method where two horizontal wells are drilled into the bitumen reserve, one of the wells is drilled a few meters above the second. Through the top well, high pressure steam is injected into bitumen reserve; this causes the viscosity of the bitumen to drop low enough so that it will flow freely to the lower well where it can then be pumped out to the surface. While this method is effective, it requires large amounts of natural gas and water to produce the required amount of steam for extraction. This makes this method more expensive to produce the same quantity and quality of crude oil as the open pit method. As such, if open-pit mining is a viable option it is the preferred method. As more subsurface reserves are found and as the surface bitumen is exhausted these and similar methods will become increasingly important in the future of bitumen extraction from the Alberta oil sands[10].

Sulphate-reducing bacteria are bacteria that obtain energy by oxidizing organic material through the reduction of sulphate. This can be an issue in the composite tailings if the bacterial community begins oxidizing molecular hydrogen to H_2S. Phospholipid analysis can be performed to monitor changes in the bacterial community present. The majority of the phospholipids present can be found within cellular membranes and as such can be used as a tool to help to identify bacterial community changes occurring across samples. Within the composite tailing samples the phospholipid profiles are expected to tie in directly to the bacteria present and can be used to illustrate any changes occurring within the phospholipid containing bacteria from sample to sample. While it is possible to monitor the entire lipidome, it is beyond the scope of this thesis. Based on work done by Harwood and Russell (1984) and Ratledge and Wilkinson (1988)[11,12], a major component of the lipid profiles of Eubacteria, Cyanobacteria and Archaea are

phospholipids and as such monitoring the phospholipid profiles should be adequate for the profiling of changes occurring within the bacterial community in the water and sediment samples.

1.3 Introduction to Lipidomics

All living organisms are comprised of cells[13]. A large number of these organisms are made up of only one cell (unicellular) and must be able to carry out all the functions necessary for life in that one cell. Bacteria, archaea, protozoa and certain algae and fungi are unicellular and while each type of organism has unique traits such as nuclei in eukaryotes and other specialized organelles, one of the constants that all cells possess a lipid bilayer which separates the contents of the cell from its surroundings. These bilayers are composed of a multitude of complex lipids which can include phospholipids, sphingolipids as well as other classes of lipids. The composition of the cell bilayer will have a dramatic effect on the structural properties and general health of the cell. While most organisms do possess a limited ability to synthesize specific lipids from simple nutrients, the primary source of lipids for most cells are obtained via transformation of complex hydrocarbon sources from the diet or from the environment. By simply changing the lipids available for uptake in mammalian cells A. Spector and M. Yorek were able to show dramatic changes in membrane function and fluidity[14]. When Ehrlich ascites tumor cells are enriched with polyunsaturated fatty acids for example, there is a 60% reduction in the α-aminoisobutyrate uptake[15], α-aminoisobutyrate is an amino acid analogue that is used as a model for short-chained neutral amino acid transport in eukaryotic cells. M. Szamel and K. Resch were also able to show large variations in membrane enzyme activity with modification to

the lipids available to lymphocytes cells[16]. Organisms themselves also change the composition of their cellular membranes depending on various stress factors that they may face in a given environment; an example of this is the incorporation of unsaturation in the fatty acid tails of phospholipids during colder periods[17]. The unsaturation within the cellular membrane increases the fluidity to keep the cell at an optimal rigidity/fluidity. A decrease in temperature by 10 to 15°C was shown to cause cyanobacteria to cease cell growth and the synthesis of new fatty acids and a dramatic increase in the desaturation of fatty acids within the membrane[18]. Similar shifts in the unsaturation of the fatty acid tails were also observed by Petersen and Klug (1994) when observing the fatty acid profiles of soil microbial communities when stored at 4.5°C, 10°C and 25°C over the course of three weeks[19]. These rapid and detectable changes to the lipid profiles of organisms have allowed researchers to perform targeted analysis to discern changes to organisms on a metabolomic level.

Metabolomics is the comprehensive study of all small organic molecules, known as metabolites, found within a given organism of interest. Metabolites are representative of both environmental and nutritional factors and also of genomic, transcriptomic, and proteomic activities within an organism[20].. The first use of the term "metabolome" was in 1998 by Oliver et al. who defined it as "the qualitative and quantitative collection of all low molecular weight molecules present in a cell that are participants in general metabolic reactions and that are required for the normal function of a cell"[21]. The term lipidomics was first used by G. Lindblom in 2002 and defined in 2003 by Gross and Han as "Lipidomics is focused on identifying alterations in lipid metabolism and lipid-mediated signaling processes that regulate cellular homeostasis during health and disease." As such, lipidomics is a sub-discipline of metabolomics focused only on lipid based metabolites.

Figure 1.2 illustrates, based on a key word search “lipidomics” is a steadily increasing field with a total of 1,110 publications since 2002.

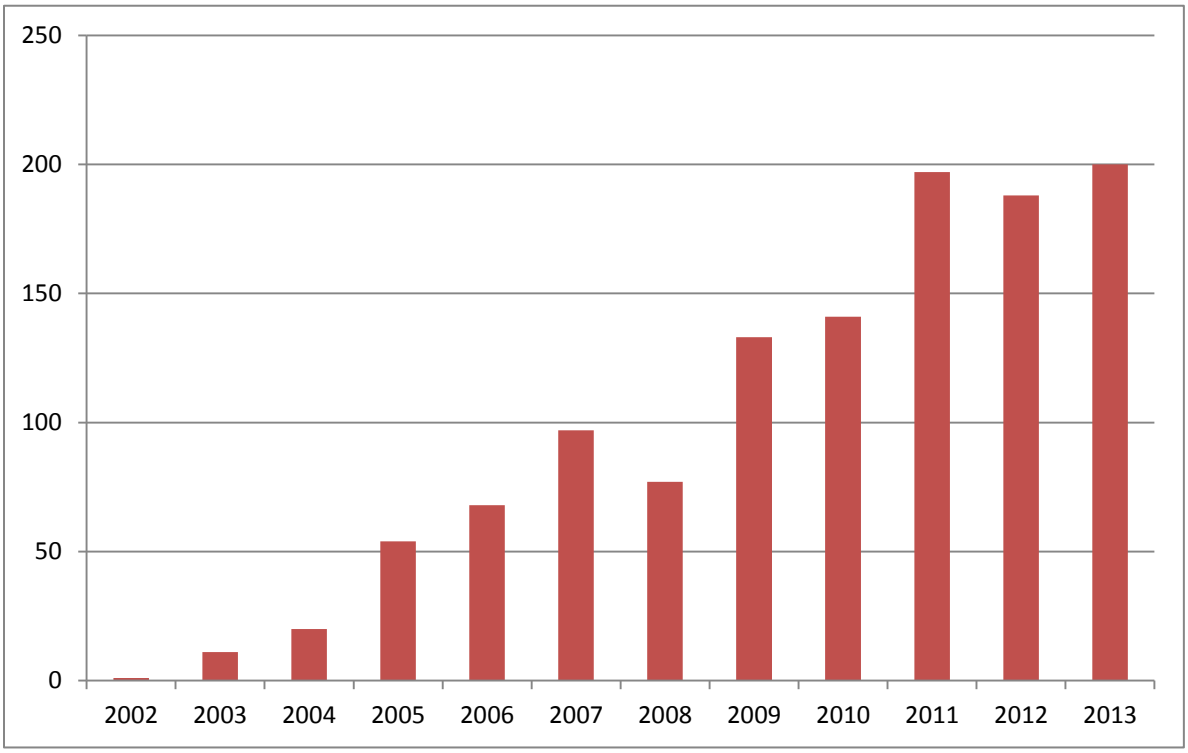

Figure 1.2 - Number of publications containing the keyword "lipidomics" as of December 5th, 2013 as per Web of Science

1.4 Structure and Naming of Lipids

While the field of lipidomics only focuses on a subset of the total metabolome, there still exists a reasonably large chemical diversity within naturally occurring lipids ranging from simple fatty acids to complex phospholipids and sterols. Figure 1.3 illustrates and defines some of the common classes of lipids while Figure 1.4 outlines the structural diversity of phospholipids, which is the main area of focus for this thesis. The naming convention for phospholipids consists of two parts; the first is a two letter abbreviation for the head group, listed in Figure 1.4, whereas the second is a numbering system for the hydrocarbon tail units. The tail unit numbering system has two forms and an example is shown in Figure 1.5, the first form is X:Y where X is the total number of carbons in both tail units combined and Y is the degrees of unsaturation found within both tail units. The second method has the form M:N/R:S where M is the number of carbons on the first tail unit and N is the number of degrees on unsaturation of the same tail, R is the number of carbons on the second tail and S is the number of degrees of unsaturation.

The naming of phospholipids with ether linked tails follows the same rules as those with ester linkages however the tail containing the ether linkage is followed by an “e” to denote the ether linkage. From above M:N/R:S would denote the ester linked phospholipid, while M:Ne/R:S would denote the corresponding ether linked phospholipid.

Lipid Class	Generic Structure	Variations
Fatty acids	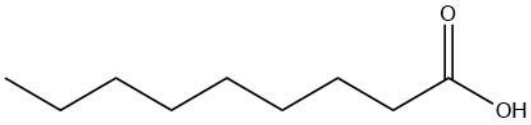	- Acyl chain varies greatly in length - Acyl chain may contain varying degrees of unsaturation
Triglycerides	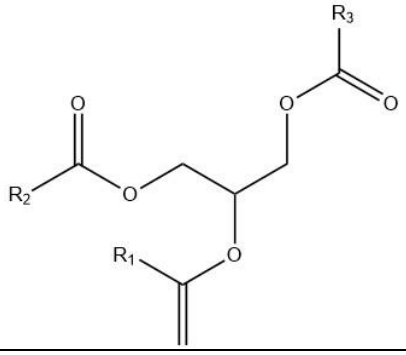	- R groups do not need to be identical and can vary greatly in length - R groups can have varying degrees of unsaturation
Phospholipids	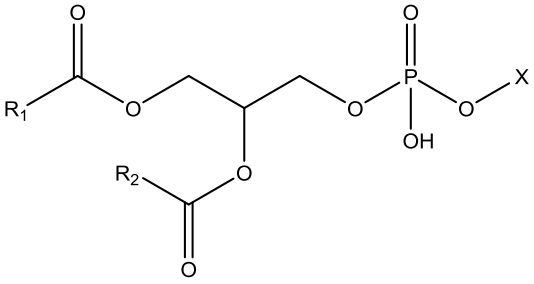	- R_1 and R_2 are typically acyl chains of varying length - X is known as the head group, chemical properties can vary greatly depending on the head group present
Sphingolipids	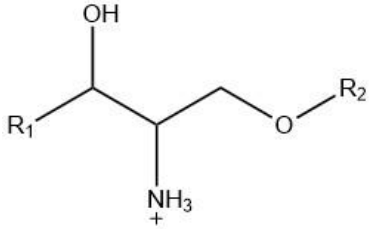	- Amine group can contain a fatty acid residue - R_1 is typically an acyl group with varying length and unsaturation - R_2 can contain similar head groups to phospholipids or a proton (alcohol)

Figure 1.3 - Structure and variations of common lipid classes

<table>
<tr><td colspan="4">Phospholipid Structure
 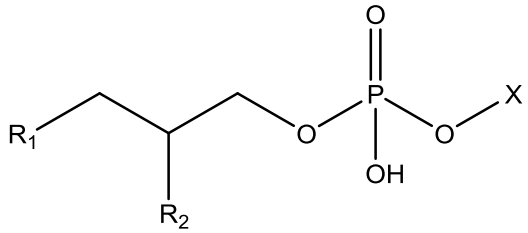 </td></tr>
<tr><td colspan="2">Head Groups (X)*</td><td colspan="2">Tail Units (R_1 & R_2)*</td></tr>
<tr><td>Ethanolamine (PE)</td><td> 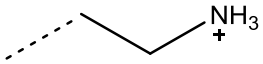 </td><td rowspan="2">Ester linkage</td><td rowspan="2"> 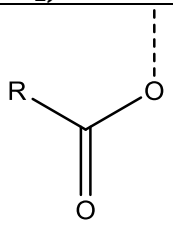 </td></tr>
<tr><td>Choline (PC)</td><td> 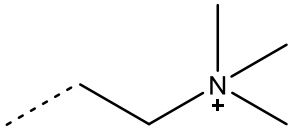 </td></tr>
<tr><td>Acid (PA)</td><td>-H</td><td rowspan="2">Ether linkage</td><td rowspan="2"> 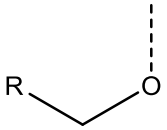 </td></tr>
<tr><td>Serine (PS)</td><td> 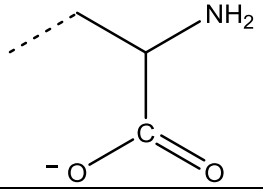 </td></tr>
<tr><td>Inositol (PI)</td><td> 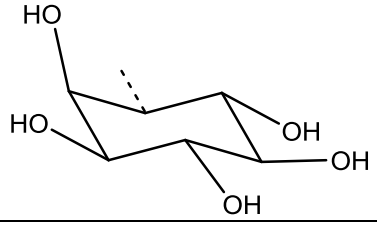 </td><td rowspan="2">Lyso</td><td rowspan="2">-OH</td></tr>
<tr><td>Glycerol (PG)</td><td> 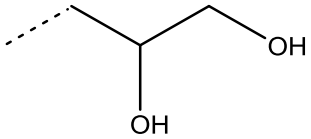 </td></tr>
</table>

Figure 1.4 - Detailed Structure of phospholipids

*dashed lines denote the bond to the R/X group in the figure of the general structure

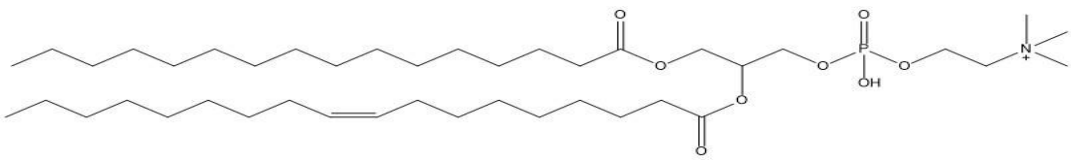

Figure 1.5 – 1-palmitoyl-2-oleoyl-sn-glycero-3-phosphocholine, known as PC 34:1 or PC 16:1/18:0

1.5 Current Analytical Techniques for Phospholipid Analysis

While there are a number of analytical techniques available for the analysis of phospholipids, by far the most common involve the use of mass spectrometry (MS). Two such techniques are high performance liquid chromatography (HPLC) coupled to MS and phospholipid fatty acid methyl ester analysis by gas chromatography coupled to MS.

Both of these techniques involve a separation step prior to MS detection which has the advantage of providing complementary data in the form of retention time which adds additional selectivity and reduces the potential of matrix interferences which may contribute to measurement inaccuracy. While GC offers excellent separation, this technique requires extensive sample preparation including the cleavage of the fatty acid component of the lipid and the chemical derivatization of the fatty acid, typically esterification into the methyl ester in order to provide sufficient volatility for separation. Due to this limitation, intact lipids cannot be directly measured by GC-MS. Alternatively, reversed phase HPLC allows for the determination of intact lipids since no chemical derivatization is required for separation. However, due to the extremely hydrophobic nature of most lipids, run times in reversed phase are typically long and the methods often require extensive optimization to provide high quality data. Due to the lower throughput of these methods and the technical difficulty of optimization of the chromatographic methods, it was decided that GC and LC separation were not ideal as a primary screening technique with respect to this thesis.

Direct infusion mass spectrometry relies entirely on the mass spectrometer to be able to distinguish phospholipids from other unknowns in the sample either through exact mass identification or multi-dimensional mass spectrometry. It has been previously shown that the major classes of phospholipids can be distinguished by specific neutral loss mass spectrometry

and precursor ion scan mass spectrometry[22–26]. This is possible because each class of phospholipid has a unique head group that can either be lost as a neutral or will fragment as ions, which can be observed by neutral loss and precursor ion scan modes respectively as described in the MS/MS section. The probability that another compound will also fragment to produce the same neutral loss or precursor ion is quite low as it would require another molecule to contain an isobaric moiety that can undergo similar fragmentation. As such it can be assumed that the signals present are only caused by the specific class of phospholipid. Furthermore, since there are metabolic pathways within organisms to convert a phospholipid of one class to another class based on its needs, for example, an ethanolamine head group can be methylated to a choline head group via the phosphatidyl ethanolamine methyltransferase enzyme, patterns can arise where phospholipid of different classes contain the same fatty acid tail units. As such patterns arise where phospholipids will only differ by the mass difference of their respective head groups. These patterns can be observed by performing the appropriate MS/MS analysis for each lipid class. When these patterns are present it is further evidence for the positive identification of MS signals at the LOD as the appropriate phospholipids. One of the main advantages to direct infusion mass spectrometry is that since there is no separation prior to the mass analyzer the sample throughput is greatly increased compared to LC and GC methods.

1.6 Introductory to Mass Spectrometry

A mass spectrometer is an instrument capable of separating molecules based on their exact monoisotopic mass to charge ratio (m/z). All mass spectrometers have three common components; an ionization source, a mass analyzer, and an ion detector. The ionization source, located at the front end of an MS system is responsible for producing ions to be analyzed. The most common ionization sources for lipidomics, and as such those of interest for this thesis, include electron impact ionization (EI), atmospheric pressure chemical ionization (APCI), matrix assisted laser desorption ionization (MALDI), and electrospray ionization (ESI). Figure 1.6 shows the range of polarity and molecular masses for which the given ionization method is useful[27].

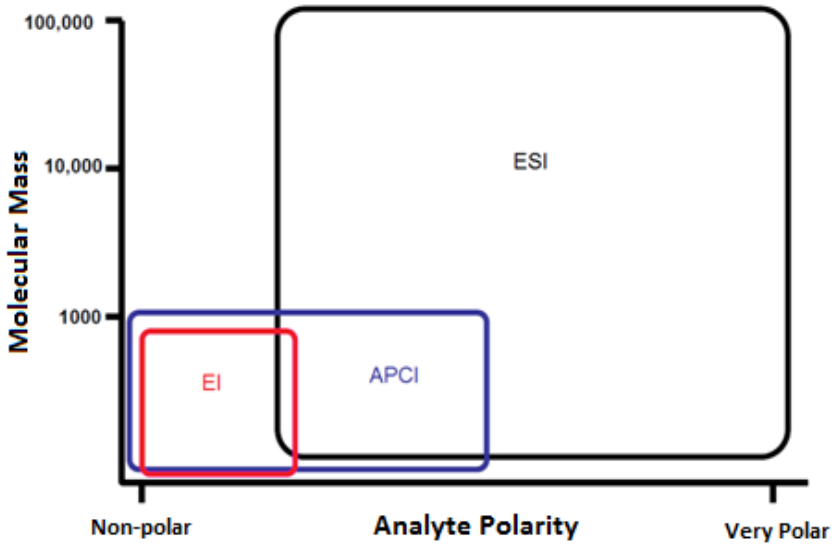

Figure 1.6 Comparison of three of the most commonly used ionization methods for lipidomics analysis[19]

Electron Impact ionization is a high energy or "hard" ionization method which imparts a significant quantity of energy to the molecule; this large amount of internal energy is usually sufficient to break chemical covalent bonds within the molecule which results in fragmentation. This fragmentation can provide structural information of a given molecule and by piecing together the fragment pattern it is potentially possible to discern the structure of the molecule. This method is most suited to high volatility samples, since the analyte must be in the gas phase to be ionized, and is most often coupled to a gas chromatograph. When electron impact ionization is used for complex samples chromatographic separation is almost always required due to the complexity of the resulting spectrum when the fragmentation pattern of all analytes is considered. In the field of lipidomics the analysis of fatty acid methyl esters (FAMEs) is most often accomplished by GC-MS using an EI source[28–31]. Intact phospholipids cannot be analyzed with this technique due to their low volatility.

APCI is a chemical ionization method where a gas, typically nitrogen in the presence of water vapour is ionized by coronal discharge. This charged gas then undergoes multiple gas-phase reactions to mainly produce a solvated proton, $H^+(H_2O)_n$, this then comes in contact with the gas-phase analyte and transfers a proton. This technique imparts significantly less energy than EI and as such results in significantly less fragmentation. This technique still has similar draw backs for lipidomics in that the sample requires some degree of volatility and requires that the analyte be thermally stable, with temperatures between 350-500°C being required[32,33]. As such APCI is not a common technique used for the analysis of phospholipids although it may be useful for other lipid classes such as intact tetraether lipids found in Archaea.

MALDI is a soft ionization method used extensively for spatial imaging of proteins and other macromolecules and for the analysis of large molecules such as polymers. The mechanism for the ionization of the analyte is a two-step process. The sample is loaded within a matrix compound that absorbs UV laser light, such as 2,5-dihydroxy benzoic acid or 3,5-dimethoxy-4-hydroxycinnamic acid. A UV laser is then fired at the matrix; the matrix will absorb the laser energy and is desorbed and ionized by the addition of a proton. The second step of the process is the proton transfer from the matrix to the analyte resulting in an $[M+H]^+$ analyte ion. This proton transfer is not limited to a single event and can lead to multiply charged species. This technique has been shown to have great spatial resolution and has been used to show variations in lipid profiles across a given sample[34–37]. Although it is effective for observing many lipid classes, MALDI is often technically challenging to reproduce and as such is not routinely used for quantitative analysis.

1.7 Electrospray Ionization

Electrospray ionization is the most widely used technique for the analysis of intact phospholipids. It was first reported in 1937 by Chapman when he was able to detect "gas-phase ions from spraying an electrified salt solution from a metal tube"[38]. Since then the method has been improved and various models have been presented as to the mechanism of ionization. The two leading theories are the "ion evaporation" model first presented by Iribarne and Thomson[39] and the "free-jet" model, also known as the Coulombic fission model, presented by Dole[40].

Both the ion evaporation and the free-jet/Coulombic fission begin with the analyte molecules first becoming chemically ionized through the addiction or loss of an ion in solution forming adducts. This solution is then sprayed from a capillary tube under an applied voltage creating an electrospray. It is from this point forward that the two models differ. The first, ion evaporation, illustrated in Figure 1.7, predicts that as the droplet evaporates and decreases in size, the surface will become increasingly crowded with charged ions. Once the droplet has evaporated sufficiently, the Rayleigh limit will be reach meaning the force from the droplet surface tension will be equal to the Coulombic repulsion of the ions and the ions will separate from the droplet and evaporate into the gas phase.

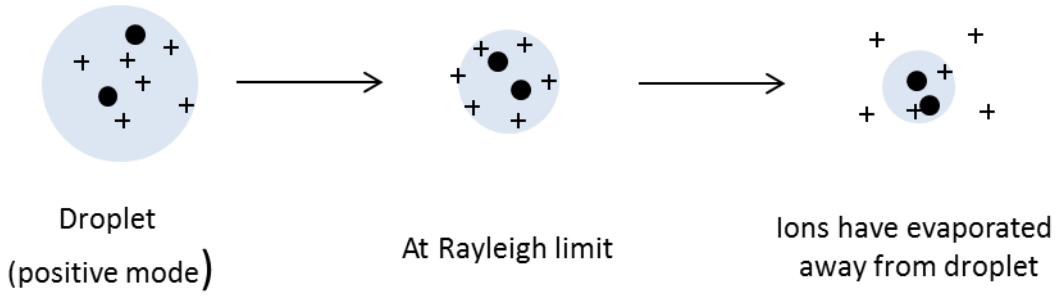

Figure 1.7 - Ion evaporation model of electrospray ionization

The second model, Free-jet/Coulombic fission, illustrated in Figure 1.8, predicts that once enough of the droplet solvent has evaporated to reach the Rayleigh limit the ion-ion repulsion within the droplet with cause it to explode releasing some of the ions into the gas phase. This process of evaporation followed by droplet explosion can repeat itself as smaller and smaller droplets are formed.

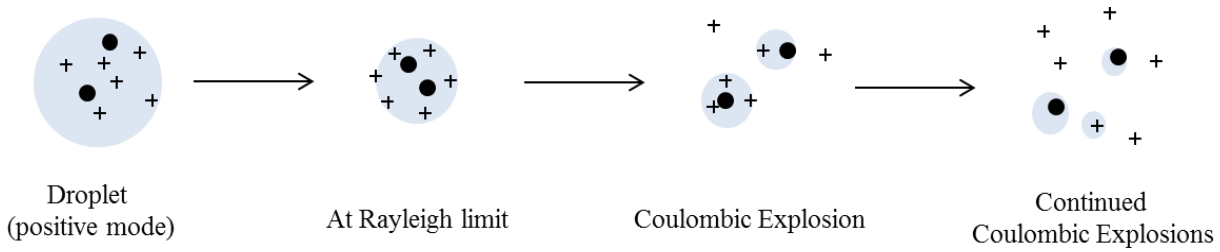

Figure 1.8 - Free-jet/Coulombic fission model of electrospray ionization

ESI is most suited to intact phospholipid analysis due to the low energy ions produced resulting in very little fragmentation. As such most compounds will be observed as a single peak in the mass spectrum. These ions are also very well suited to collision induced dissociation (CID), which for phospholipids allows for the identification of the lipid head group. ESI is also one of the few ionization techniques which do not require the analytes be volatile and thermally stable. There are still significant drawbacks to ESI, the two main ones being variation in ionization efficiency and ion suppression. Ionization efficiency refers to the rate at which one molecule will become ionized. The ionization efficiency or relative response within ESI, unlike other ionization techniques, is extremely variable and is largely dependent on the chemical structure and physicochemical properties of a given molecule. As such the ionization efficiency

of a given molecule may vary many orders of magnitude. As a result of the relative response variations observed in ESI when a sample is being analyzed it is necessary to construct a calibration curve using known standards for each molecule to be quantified. This can become quite tedious and sometimes impossible for complex unknown samples. The ionization efficiency for a given molecule can also vary greatly with instrument parameters and experimental conditions such as solvent choice and addition of various salts, ammonium acetate being a common addition to sample being analyzed[41]. This limitation forces the researcher to spend a significant amount of time initially in the optimization of these parameters prior to the analysis of samples.

The second limitation of ESI is ion suppression or enhancement. Ion suppression is a phenomenon where the presence of other ions will suppress the signal of the desired ion. This can be due to a higher concentration or simply due to higher ionization efficiency. As previously discussed in both the ion desorption model as well as in the Coulombic fission model the ions that occupy the surface of the charged droplet will be the ions that are most likely to be released into the gas-phase. As such it is clear that as the surface of a charged droplet becomes more and more crowded with ions the surface will become saturated and a maximum number of ions will be released regardless of the true concentrations within the droplet. The result is a negative bias representation of the ions present in the solution. Similarly ion enhancement occurs when chemical interferences cause an increase in response compared to what is normally seen without sample matrix. Ion suppression/enhancement can be overcome through various experimental parameters, for example a sample cleanup step may be required to remove excess salts from solution, introducing a separation method prior to MS analysis, or simply by lowering the total ionic strength by diluting the sample[42].

1.8 Introduction to Mass Analyzers used in phospholipid analysis

The mass analyzer is the component of a mass spectrometer in which the ions are separated based on their mass to charge ratio (m/z). In lipidomics, the critical performance characteristics of a mass analyzer are their mass accuracy and resolution as well as the ability to perform CID experiments. There are other characteristics to take into account such as linear response range and ease of use that must be taken into account when choosing a mass analyzer. Figure 1.9 shows a general overview of a large variety of commonly used mass analyzers.

	Mass Analyzer						
Characteristic	Magnetic Sector	Triple Quadrupole	Ion Trap	Orbitrap	Time-of-flight	Q-TOF	FT-ICR
Mass Range	~15000	~4000	~10^5	~10^5	Unlimited	Unlimited	>10^6
Mass Resolution	200,000	Unit	~100-1000	50,000-100,000	10,000-70,000	10,000-70,000	>10^6
Dynamic Range	10^5	10^6-10^7	10^5-10^6	10^4	10^4	10^4	10^4
MS/MS	Good	Good	Excellent	Excellent	N/A	Limited	Poor
Ability to couple to Separation	Low	High	High	Low	High	High	Low
Relative Cost	High	Low	Low	High	Moderate	Moderate	Very High
Ease of Use	Difficult	Easy	Easy	Difficult	Moderate	Moderate	Very Difficult

Figure 1.9 Commonly used mass analyzers and their characteristics (adapted from DASS; "Principles and Practice of Biological Mass Spectrometry" Wiley Interscience New York 2001). (Q-Tof=quadropole-time-of-flight; FT-ICR=fourier transform - ion cyclotron resonance)

All of these properties must be taken into account when choosing the proper platform to perform any experiment. For example, with direct infusion lipidomics, the mass analyzer is required to be able to perform neutral loss and precursor ion scan MS/MS experiments that cannot be directly performed on a TOF instrument despite its excellent mass accuracy and resolution. Due to its low cost, its good ability to perform CID, and its excellent quantitative properties including linear range and sensitivity, a triple quadrupole (QQQ) analyzer is the most commonly used for lipidomics.

1.9 Multi-dimensional Mass Spectrometry by QQQ-MS

Multi-dimensional mass spectrometry is a technique whereby the initial analyte ion is separated based on m/z, then enters a collision cell and fragments and the fragments are then separated once again based on m/z. This technique can be used to elucidate structural information or to help identify an unknown analyte.

Using a QQQ mass spectrometer there are three multi-dimensional techniques available. The first is product ion scan, also known as daughter ion scan, illustrated in Figure 1.10a. It is a technique where the first quadrupole is set on a specific m/z, ions of that m/z will then enter the second quadrupole, the collision cell, and be fragmented and the final quadrupole will scan a set range of m/z and detect the fragmentation of the initial ion. This technique is useful for determining structural information from a molecule of interest with a known molecular weight. The resulting spectra will show the fragmentation pattern for a given m/z.

The second method is precursor ion scan, also known as parent ion scan, illustrated in Figure 1.10b. It is a technique where the first quadrupole scans a given m/z range, ions enter the collision cell and are fragmented and the final quadrupole is set on a given m/z. The resulting spectra will represent all molecules that fragment to give a specific fragment ion. This technique is useful when determining which ions have particular functional groups or moiety.

The final method is the neutral loss scan, illustrated in Figure 1.10c. It is a technique where the first and third quadrupoles are scanned with a specific offset, for example the first quadrupole will scan a given m/z higher than the third quadrupole. The ions will enter the collision cell after being separated in the first quadrupole and undergo fragmentation before entering the final quadrupole. This technique will produce a spectrum where molecules that lose a specific neutral species are identified.

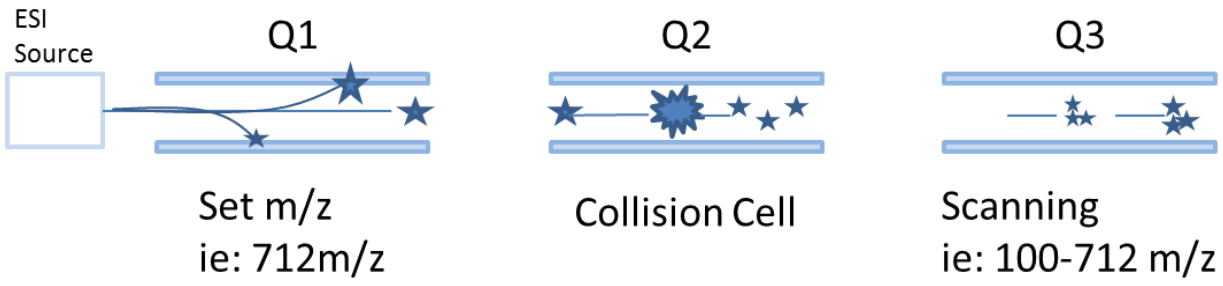

Figure 1.10a - Visual representation of product ion scan mode

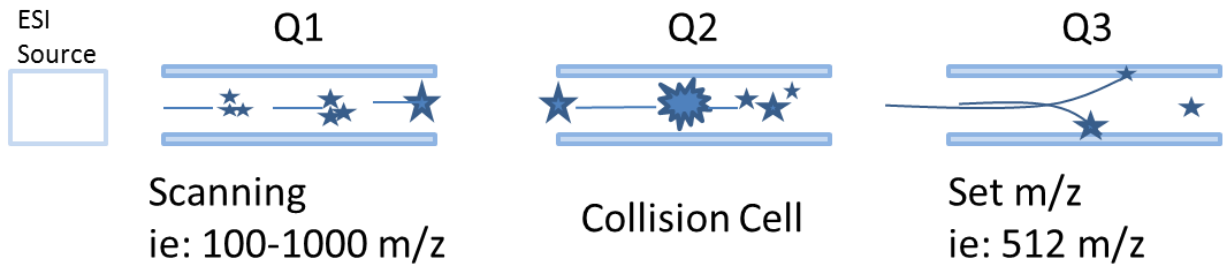

Figure 1.10b - Visual representation of precursor ion scan mode

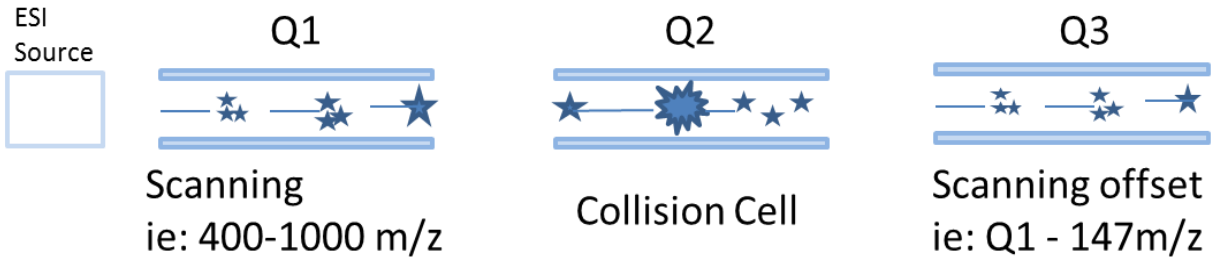

Figure 1.10c - Visual representation of neutral loss scan mode

In addition to the multi-dimensional techniques described above, there is also the potential for multiple reaction monitoring, MRM. Unlike single reaction monitoring, SRM, where one analyte is observed through any of the three methods described above, MRM instead monitors multiple analytes by switching modes and/or parameters after each individual scan. This allows a QQQ to simultaneously analyze the phospholipids that ionize to the same charge (positive or negative)

Thesis Objectives

The overall goal of this thesis was to optimize a direct-infusion lipidomics method previously developed by Libia Saborido Basconcillo[24,25] for the analysis and quantify of phospholipids present in both water and sediment samples. The end goal was to apply this optimized method to samples collected from a Syncrude composite tailing site. The specific objectives to accomplish these goals and outlined within this thesis are:

1. To investigate the addition of adduct forming salts that are expected to increase the fragmentation efficiency of phosphatidylethanolamine and phosphatidylcholine,
2. To investigate and optimize mass spectrometry parameters,
3. To optimize current methods for the extraction of phospholipids from both water and sediment samples contaminated with bitumen and other oil byproducts,
4. To assess the suitability of direct-infusion lipidomics as a tool for the identification and quantification of water and sediment samples,
5. To assess the changes in the phospholipid profile occurring within Sandhill Composite Tailings fen water samples both temporally across a one year period and spatially both vertically and horizontally across the fen,
6. To assess the changes in the phospholipid profile occurring within Sandhill Composite Tailings fen sediment samples both temporally across a one year period and spatially across the fen at different locations but similar depths.

.

Chapter 2: Methods and Materials

2.1 Equipment and Chemicals

Chemical standards and solvents

Solvents used for the extraction of phospholipids from both water and sediment samples were HPLC grade methanol, chloroform, water and dichloromethane from Caledon Laboratories. Phospholipid standards were obtained from Avanti Polar (Alabaster, Alabama). A full list of all phospholipid standards used can be found in Appendix 1.

Mass spectrometer

Throughout this thesis the primary MS instrument that was used was a Waters Quattro Ultima Triple Quadrupole instrument equipped with a Waters Micromass fused silica capillary. The mass calibration was confirmed during each experiment using an internal calibration standard consisting of one phospholipid from each class being analyzed.

2.1.1 Other Instruments

For all methods, chemical standards were weighed on a Mettler AC 100 series analytical balance and pH of phosphate buffer for the modified Blight and Dyer extraction was measured with a pH209 series bench top pH meter. For methods requiring the pelleting of suspended material a Labnet bench top centrifuge was used.

2.2 MS Parameters

Figure 2.1 shows the MS parameters used to obtain mass spectrum of phospholipids.

Lipid Class	Mass Range (m/z)	Collision Energy (eV)	Scan Time (s)	MRM Type	MRM m/z	ESI Mode
PE	450-1000	30	1.5	Neutral loss	147	Positive
PC	450-1000	35	1.5	Neutral loss	189	Positive
PS	450-1000	25	5	Neutral loss	87	Negative
PI	450-1000	35	5	Precursor ion	241	Negative
PG & PA	450-1000	25	5	Precursor ion	153	Negative

Figure 2.1 - Mass Spectrometer parameters used for the acquisition of mass spectrum of phospholipids

2.3 Data Processing and Extraction

All MS spectra were first processed using Mass Lynx (version 4.0) software to obtain peak area data using the following procedure. First, the spectra are combined excluding any scans that produced noise peaks that interfere with analyte signals. Second, the combined spectrum is smoothed four times using mean smoothing method with a peak width of 0.75. Third the smoothed spectrum is background subtracted using a polynomial order of 5. Finally, the background subtracted spectrum is centered using centroid of top 80% method for peak areas. Calibration curves for thirteen positive mode phospholipids, PC and PE, and thirteen negative mode lipids, PG, PI, PA, and PS, were constructed using an Excel based program originally developed by Yemi Sofowote and modified for this application. A second Excel based program

was developed for this thesis to then extract phospholipid concentrations from the unknown samples based on the constructed calibration curves and isotope peak identification for confirmation of a real signal. Finally phospholipids could be identified based on MS/MS fragmentation data using a third Excel based program developed to provide theoretical fatty acid tail formulas based on the fragmentation pattern present in an individual phospholipid.

2.4 Statistical Analyses

Principal component analysis (PCA) and orthogonal partial least squares-discriminate analysis (OPLS-DA) were performed using the data analysis software package SIMCA P+ (version 13.0.3). For all analyses Pareto scaling with a 1/square root block weight was applied.

2.5 Water and Sediment Sample Collection, Preparation, and Extraction

All water and sediment samples for this thesis were collected by the Dr. Lesley Warren group of McMaster University. The samples were collected at Syncrude's Mildred Lake Settling basin. The sediment samples were collected between 10-30 centimeters below the sediment surface. Initially sediment was shovelled out of the ground, then using a sterilized silicone spatula sediment was scoop, careful not to take sediment in contact with the shovel, into sterile Whirlpak bags or carbon-free glass jars. All equipment and gloved hands were sterilized with 70% ethanol immediately prior to sample collection. Any air in the sample bags was expelled

and the samples were sealed and stored in a cooler on ice for the remainder of the day and stored at -20°C as soon as possible until analysis[43].

Groundwater samples were collected from monitoring wells installed within the Sandhill Fen Reclamation site. The well locations are shown in figure 2.2 and 2.3. Well depths ranged from 10.97 to 26.47 meters below ground surface. Water samples were collected from the polyethelyene tubing and inertial lift pump system (Waterra) and into pre-cleaned plastic Nalgene bottles. The water samples were stored in a cooler on ice for the remainder of the day and stored at -20°C when possible until analysis[43].

Figure 2.2 shows an overview of the Syncrude Mildred Lake Settling Basin along with the Sandhill Fen and Kingfisher Fen. Figure 2.2 shows the well locations within the Sandhill Fen where both water and sediment samples were taken. Figure 2.3 depicts the relative depths of each well and the depths of the sand cap and composite tail.

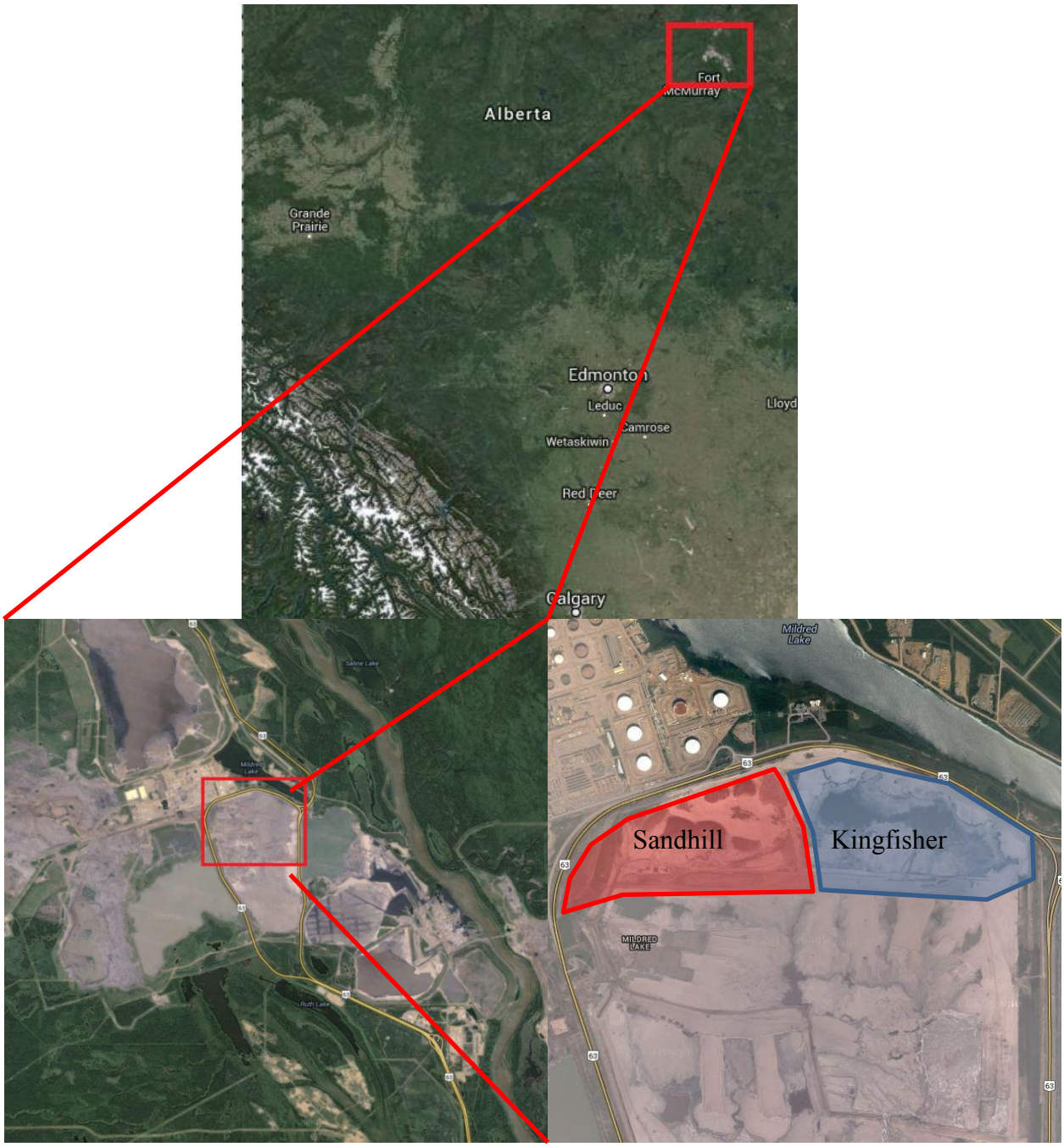

Figure 2.2 - Top: Map of Alberta depicting the location of the Syncrude mining site

Bottom Left: Mildred Lake Settling Ponds and Composite Tailings Fens

Bottom Right: Sandhill Fen and Kingfisher Fen locations

Source: Dr. Warren et al. and Google Maps

Figure 2.3 – Locations of the sampling wells within the Sandhill Fen

Source: Dr. Warren et al

Well Name	Depth	Final Layer
6A	8m	Sand Cap
Sump Vault	10m	Interface of Composite Tailings and sand
5D	15m	Composite Tailing
8C	24m	Composite Tailing

Figure 2.5 - Depths and final layer locations of the sampling wells in the Sandhill fen

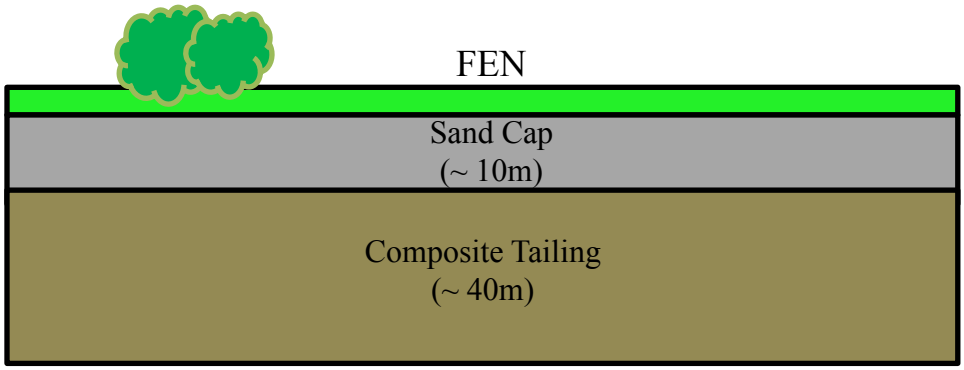

Figure 2.4 - Sandhill Fen cross section

Source: Dr. Warren et al.

2.6 Water Extraction Methods

The water samples were stored frozen at -20°C; as such it was required to allow the samples to completely thaw before extractions. This was accomplished by leaving the Nalgene bottles at room temperature overnight prior to extraction. Two procedures were finalized for the analysis of the water samples, the first involved a classic liquid-liquid extraction of the water sample and the second involved the analysis of suspended material found within the water.

The first procedure was performed by measuring 10.0 mL of water sample and pouring this into a 60 mL separatory funnel. A recovery standard mixture containing; PA 12:0/12:0, PG 17:0/17:0, PE 8:0/8:0, PC 12:0/12:0, and PS 10:0/10:0, were added and the mixture homogenized by shaking. The water sample was then extracted a total of three times with an equal volume of chloroform (10.0 mL). The three chloroform layers were combined in a round bottom flask and rotary evaporated to a few mL. The remaining chloroform was transferred to a 0.5 dram vial; the round bottom flask was rinsed three times with 1-2 mL of chloroform and transferred to the vial. The chloroform in the vial was blow down to dryness with a gentle stream of N_2 gas. This dry extracted was then resuspended in 200 μL of 1:1 $CHCl_3$:MeOH. This final resuspended extract was then stored at -20 °C until analysis.

The second procedure was performed by measuring 2.00 mL of water sample into an Eppendorf tube. The water sample was then centrifuged for 5 minutes to separate the suspended material for the water. The water was then removed and the silt and other suspended material were resuspended in 500 μL of HPLC grade water. The same recovery standard mixture containing; PA 12:0/12:0, PG 17:0/17:0, PE 8:0/8:0, PC 12:0/12:0, and PS 10:0/10:0, was then added to the sample and homogenized by vortexing. A modified Bligh and Dyer extraction[44] was

then performed according to the following procedure. Dichloromethane and methanol were added so that a final ratio of 1:1:0.8 DCM:MeOH:H_2O was reach, the mixture was then vortexed for 1 minute and centrifuged for 5 minutes. The DCM layer was then removed and the procedure repeated for a total of three extractions. The DCM layers were combined and run through a small Na_2SO_4 plug to remove any remaining water. The Na_2SO_4 plug was rinsed three times with small volumes of DCM (0.2-0.5mL). The DCM was transferred to a 0.5 dram vial and blown down to dryness using a gentle stream of N_2 gas. The dry extract was then resuspended in 50 μL of 1:1 $CHCl_3$:MeOH and stored at -20°C until analysis.

2.7 Sediment Extraction Methods

The procedure used for the extraction of phospholipids from sediment samples was developed from a modified Bligh and Dyer procedure[44]. Between 5-20g of sediment was placed into a 250 mL beaker, 5 mL of a mixture of 1:1:0.8 DCM:MeOH:H_2O was added for every 1g of sediment. The beaker was then covered with aluminum foil and sonicated for 10 minutes then allowed to extract overnight. The resulting solution was then filtered into a separatory funnel and the DCM layer was isolated from the aqueous layer. The MeOH:H_2O layer was then extracted two more times with DCM and the DCM layers combined in a round bottom flask. The layers were rotary evaporated to a few mL, transferred to a 0.5 dram vial and blown down to dryness with N_2 gas. The resulting extract was then resuspended in the smallest volume of DCM able to dissolve the extract, typically between 1 and 2 mL. A silica column was prepared by first using a glass wool plug, one cm of sea sand, one gram of activated silica for every gram of extracted sediment sample, and finally a 1-2 cm layer of sea sand. The extract was then loaded onto the

silica column; three mobile phases were used to separate the phospholipids from other contaminants in the sediment sample. 10 mL of each mobile phase was used for every gram of silica in the column; the mobile phases used were dichloromethane, acetone, and methanol. The methanol layer contains the phospholipids from the sediment sample and was collected in a round bottom flask. The methanol was then rotary evaporated to a few mL and transferred to a 0.5 dram vial, the extract was then blown down to dryness using N_2 gas and resuspended in 0.5 mL of 1:1 $CHCl_3$:MeOH, it was then stored at -20° C until analysis.

2.8 Infusion Sample Preparation and Quattro Method

Samples were prepared for either positive mode electrospray ionization for PE and PC analysis, or negative mode electrospray ionization for PA, PG, PS, and PI analysis. Samples for positive mode ESI analysis were prepared by combining 50 μL of sample with 10 μL of internal standard, containing PE 14:0/14:0 and PC 14:0/16:0, and 5 μL of 13 mM LiCl, resulting in a 65 μL injection mixture with the $[M+Li]^+$ adduct being the major peak observed. The samples for negative mode ESI analysis were prepared by combining 50 μL of sample with 10 μL of internal standard, containing PA 10:0/10:0 and PG 12:0/12:0, resulting in a 60 μL injection mixture with the $[M-H]^-$ adduct being the major peak observed.

The mass spectrum of the samples were then acquired on the Waters Quattro using the microspray source at a flow rate of 2 μL per minute using the tandem mass spectrometry procedures outline in section 2.2.

Chapter 3: Direct Infusion Method Development

3.1 Optimization of Current Mass Spectrometry Method

Direct infusion lipidomics research has numerous obstacles and challenges to overcome prior to working on unknown samples. A method was developed using a Waters Quattro triple quadrupole mass spectrometer for comprehension lipidomics of Sinorhizobium meliloti by a previous student Libia Saborido Basconcillo[24,25,28,45]. While this method works quite well with concentrated samples of cells, water samples with an unknown concentration of cells provide a number of novel challenges for this method. The lower concentration of phospholipids in the samples requires fine tuning of the mass spectrometer parameters in order to achieve the required detection limits without introducing the issue of ion suppression that would come from further concentrating the sample either through an increase in extraction volume or a decrease in the final extract volume.

There are a large number of instrument parameters that needed to be optimized, the first of which was the mass resolution. Figure 3.1 shows the intensity of eleven lipid standards versus the resolution setting of the mass spectrometer. Based on the obtained data for the instrument in question a resolution setting of 14 on the MassLynx software for the Waters Quattro was chosen, affording a resolution of 890 at a mass to charge ratio of 712. This resulted in a width at half max of 0.8 da, although typically a target value of 0.5 is desired it was shown that variation in peak area was not sufficient to require higher resolution. The main issue being that as the resolution approached the desired value of a peak width of 0.5 at half max the intensity of twelve of the sixteen standards approached the limit of detection (LOD). As a goal of the thesis was the

identification of changes in phospholipid profiles within samples and not the absolute quantification of individual phospholipid species this was an acceptable resolution and provided the optimal detection of phospholipids. As the resolution was lowered below 890, it was noticed that the noise level within samples increased at similar rates as the phospholipid standards; as such it was not beneficially to lower the resolution beyond 890.

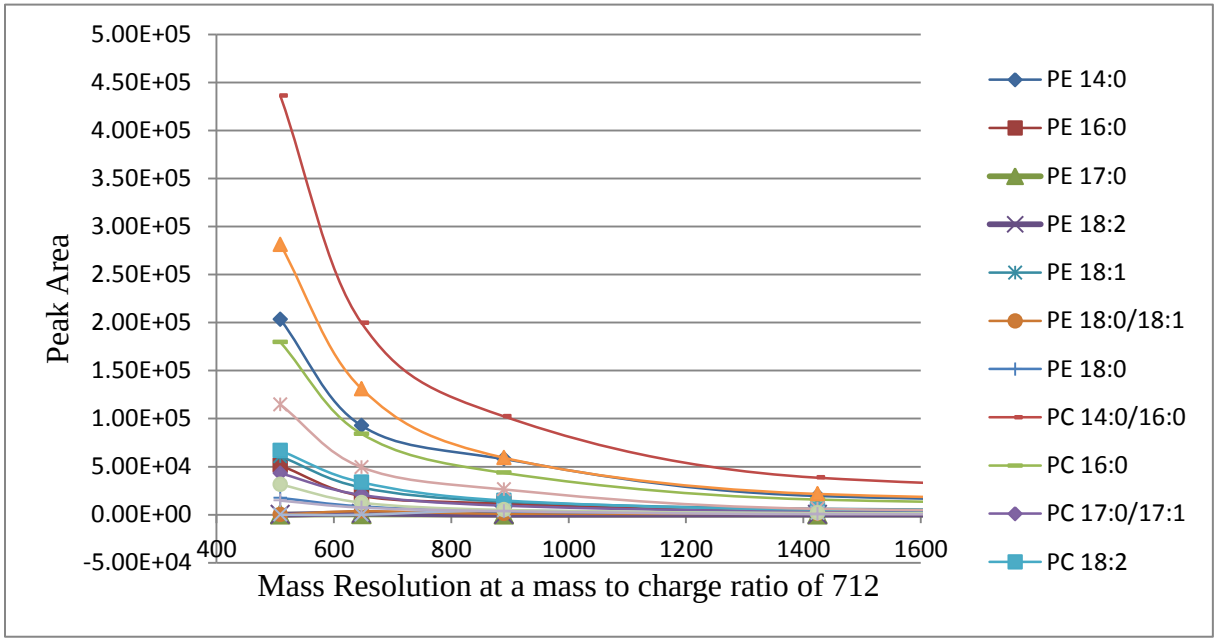

Figure 3.1 - Intensity of lipid standards versus resolution, where resolution was calculated using the PC 14:0/16:0 internal standard (m/z 712)

The second instrument parameter producing a significant variation in signal intensity was the location of the capillary from where the spray occurred with respect to the skimmer cone of the mass spectrometer. It has been shown extensively that signal quality is greatly improved by having the capillary spray orthogonally to the inlet[46], as such this variable was not explored. The distance away from the inlet was explored however and was found to greatly affect the quality of the data obtained, since this variable was one that had to be manually adjusted and could not have a value assigned it was necessary to optimize the positioning of the capillary at the

beginning of every session using a mixture of standards. With proper positioning it was possible to increase the signal to noise ratio by 1.5 times or more.

The final instrument parameter that was explored was the capillary potential, a voltage applied at the tip of the capillary to form an aerosol of highly charged droplets. It has been noted in literature that varying the capillary voltage can have an effect on the quality of the mass spectrum produced by either causing fragmentation of the analyte prior to entering the first quadrupole or by affecting the analytes ability to become an individual ion. As seen in Figure 3.2, lower capillary voltages resulted in lower signal intensities, this is due to the fact that an aerosol spray would not be fully formed and droplets would form at the tip of the capillary instead. A threshold appears to be reached at approximately 3.5 kV at which point it is assumed that there is a large enough potential to cause a sufficiently charged aerosol spray to form. Above 3.5 kV there appears to be little change in peak intensity and at the risk of causing fragmentation prior to entering the first quadrupole the cone voltage was set at 3.75 kV.

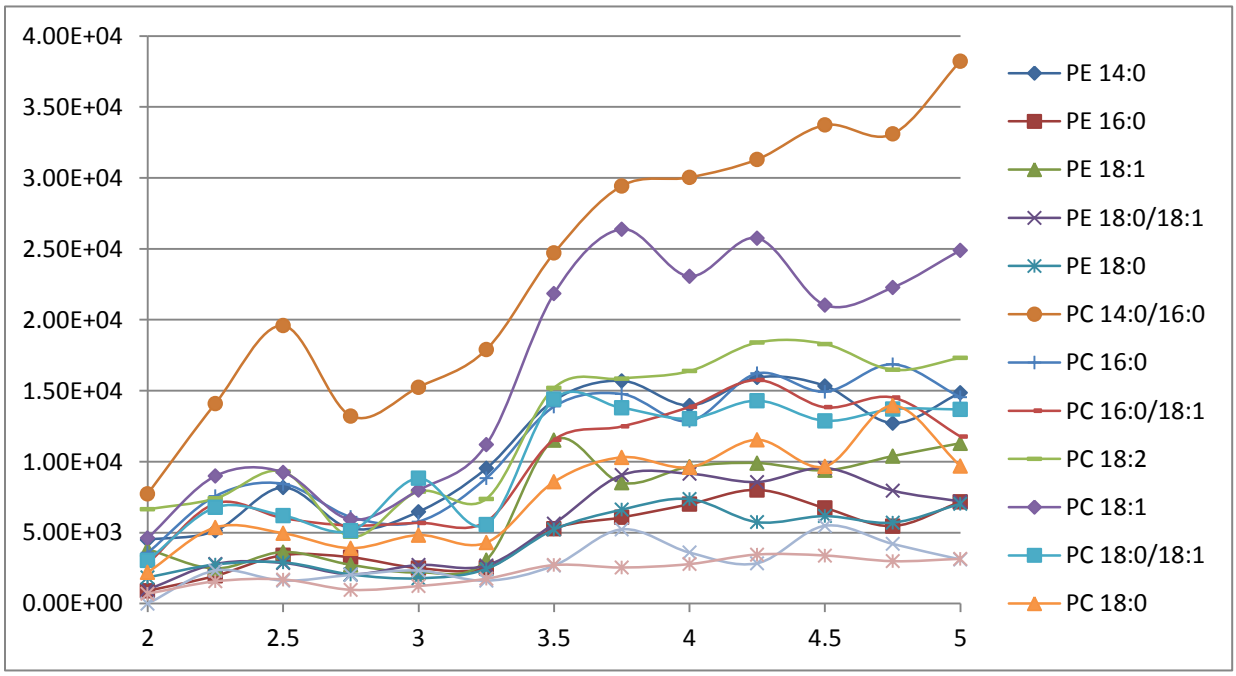

Figure 3.2 - Peak intensities of phospholipid standards versus the capillary voltage (kV)

The formation of charged adducts through the complexation or adsorption of an ion is crucial to the function of electrospray ionization. The formation of adducts not only allows for the formation of charged ions from molecules that would typically remain neutral, but also has been shown to increase the efficiency of certain fragmentations in multi-dimensional mass spectrometry. That having been said, the addition of lithium chloride (LiCl) to form $[M+Li]^+$ adducts was explored. As shown by Basconcillo et al., the addition of LiCl decreases the collision energy required for the neutral losses of the ethanolamine and choline head groups from PE and PC phospholipids[47]. Figure 4.3 shows the effects of lithium chloride concentration on the intensity of the $[M+Li]^+$ phospholipid standard signal. This figure demonstrates an increase in signal intensity as LiCl concentration increase up to an apex of 1.6 mM for almost all the phospholipid standards. This is attributed to a more efficient fragmentation resulting in a larger percentage of the phospholipids undergoing collision induced dissociation and losing the ethanolamine and choline head groups.

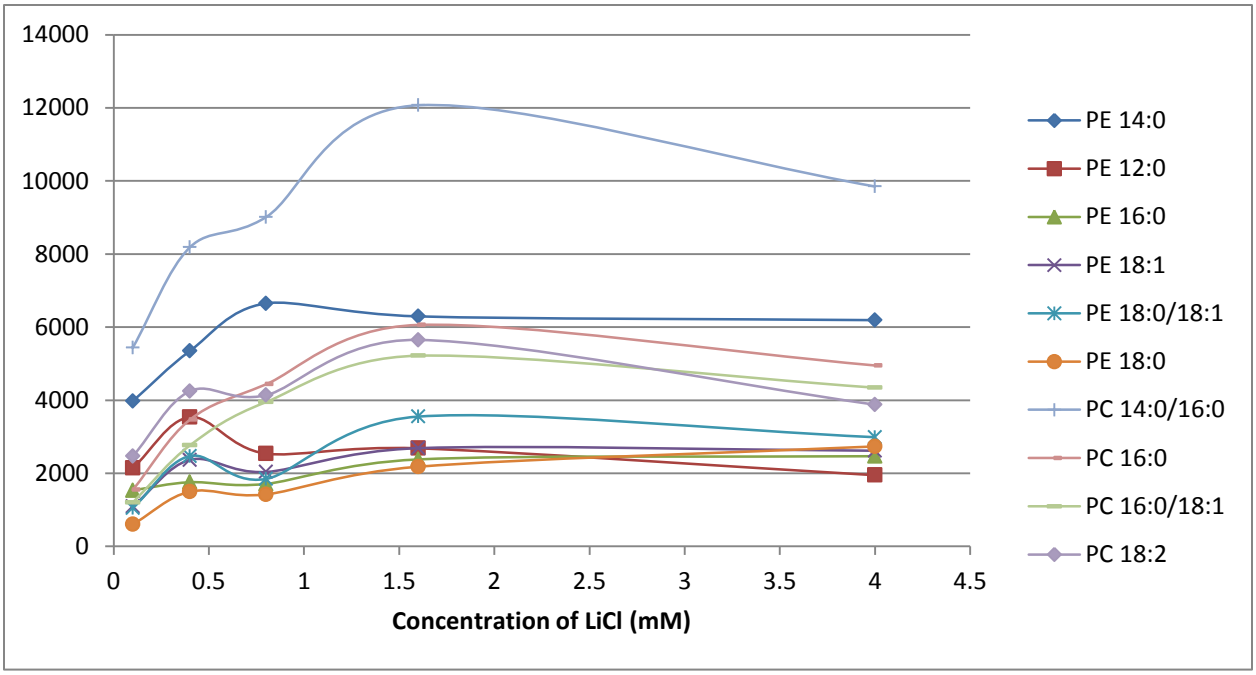

Figure 3.3 - Peak intensities of phospholipid standards versus LiCl concentration

3.2 Phospholipid Theoretical Exact Mass Database

Unfortunately there is not a publicly accessible database containing all the theoretical values for the exact mono-isotopic masses and various adduct masses for phospholipids. As such, a simple to use database containing all theoretical masses for ester linked PE, PC, PA, PS, PI, and PG lipids was developed as well as an interface for the quick and efficient search for any phospholipid based solely on whether they produce positive ion, PE and PC, or negative ions, PA, PG, PI, and PS, and also the mass of the ion. The database was created such that any common adduct mass was included and the excel file used to search for the appropriate lipid can be easily and quickly modified to search for any of the adducts that may have been formed, including $[M+H]^+$, $[M+Li]^+$, $[M+Na]^+$, $[M+NH_4]^+$, and $[M+K]^+$ for the positive mode lipids and simply $[M-H]^-$ for the negative mode lipids. Figure 3.4 shows the interface used in looking up positive mode $[M+Li]^+$ adducts based on mass. Since these lipids are identified both by neutral loss fragmentation pattern then by mass, an accurate mass is not necessary and lipids within 0.5 m/z can be easily identified.

Lipid Lookup					
Lipid Mass		Possible Matches	Masses	Difference	Abundance
712.5		PC 30:5	702.4686115	10.03138853	100
Data Location		PE 33:4	704.4842615	8.015738456	100
B378		PC 30:4	704.4842615	8.015738456	100
		PE 33:3	706.4999116	6.000088382	100
		PC 30:3	706.4999116	6.000088382	100
		PE 33:2	708.5155617	3.984438308	100
		PC 30:2	708.5155617	3.984438308	100
		PE 33:1	710.5312118	1.968788234	100
		PC 30:1	710.5312118	1.968788234	100
		PE 33:0	712.5468618	0.04686184	100
		PC 30:0	712.5468618	0.04686184	100
		PE 34:6	714.4686115	1.96861147	100
		PC 31:6	714.4686115	1.96861147	100
		PE 34:5	716.4842615	3.984261544	100
		PC 31:5	716.4842615	3.984261544	100
		PE 34:4	718.4999116	5.999911618	100
		PC 31:4	718.4999116	5.999911618	100
		PE 34:3	720.5155617	8.015561692	100
		PC 31:3	720.5155617	8.015561692	100

Figure 3.4 - Phospholipid lookup interface for positive mode lipids (PE and PC)

3.3 Phospholipid Fragmentation database

A second database was created using the theoretical exact mono-isotopic mass of the potential fragment ions of phospholipids to identify phospholipid tail units based on product ion scans. By first compiling a list of all possible tail chain lengths and degrees of unsaturation, then creating an interface to quickly search through all the possible mass losses due to fragmentation it was possible to create a quick and easy means to determine the likely structure of a phospholipid based on its fragmentation. Two search interfaces were created; the first takes an imported spectral list from the MassLynx software and compiles a list of possible tail fragments. This is done by using the mass of the whole phospholipid and the lipid lookup database in section 3.2 to determine the length of both combined tails and unsaturation then looking for every combination of tails possible fitting those totals and matching them to signals in the mass

chromatogram. If both signals are present and in reasonable ratios then a possible match is awarded, it is possible that multiple combinations return a probable match and as such it is still necessary to manually go through the possibilities to narrow it down to likely candidates.

The second search interface begins similarly by first determining the totals of both tail units, then after producing a product ion scan of the target lipid, the total phospholipid mass and the mass of one of its fragments are put into the search boxes in the interface and potential tail structures and linkages are presented. From here a second tail fragment mass is presented and by looking back at the product ion scan it is possible to identify whether or not the second fragment ion is present, confirming or denying the first identification. Figure 3.5 depicts a product ion scan of a known phospholipid, PC 16:0/14:0 with the losses of the tail units highlighted. Figure 3.6 shows how using the total mass and the mass of one of the fragment ions, in this case 712.41 and 484.28 respectively, the identities of the tail units are confirmed.

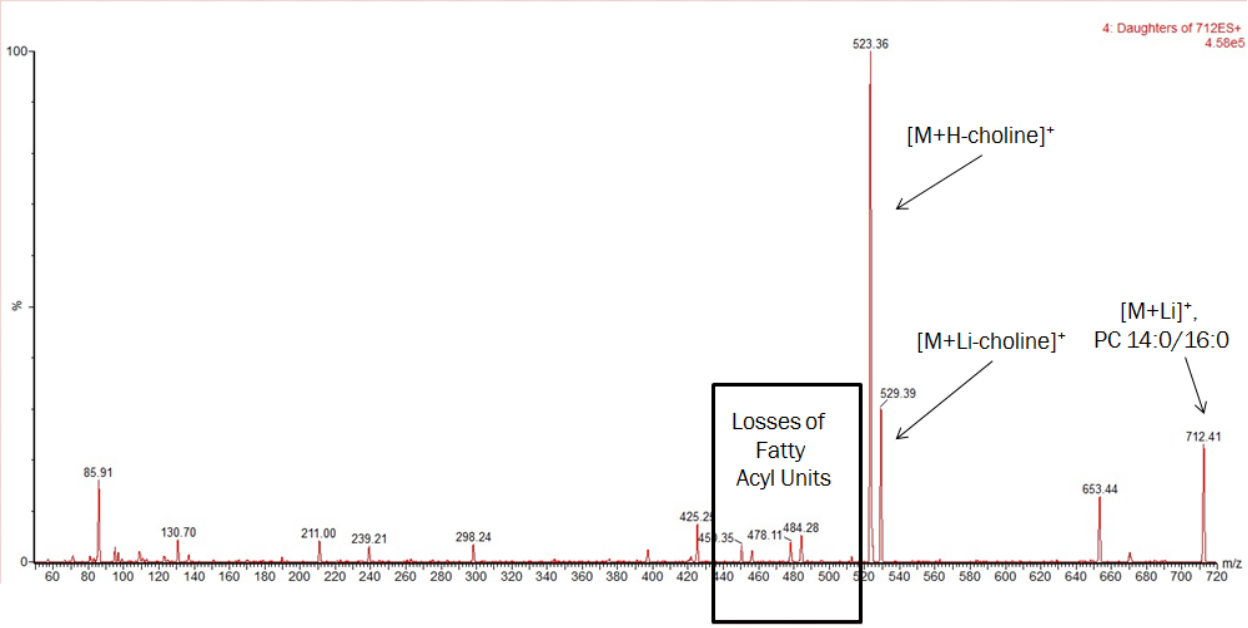

Figure 3.5 - Product ion scan of m/z 712, PC 16:0/14:0, highlighting the loss of the tail units

		Tail Loss Lookup						
Lipid Mass	712.41	Loss Seen	Possible Matches			Masses	Loss Seen	Difference
Frag Mass	484.28	228.13	Link ID	Chain Length	Unsat			
		Data Location	OH	17	8	226.1721508	227.1799759	0.950024149
PE: 0 PC: 1	1	E993	Am+OH	14	1	226.2170897	227.2249147	0.905085279
			Diol	15	2	226.2296658	227.2374908	0.892509213
			ES	15	0	226.2534752	227.2613002	0.868699771
			OH	16	1	226.2660513	227.2738763	0.856123705
			ES	15	7	227.1072048	228.1150299	0.014970128
			ET	16	7	227.1435903	228.1514154	0.02141538
			ES	14	0	227.2011053	228.2089303	0.078930316
			ET	15	0	227.2374908	228.2453158	0.115315824
			Am+OH	15	7	228.1388393	229.1466644	1.016664351
			Diol	16	8	228.1514154	229.1592404	1.029240417
			Amine	16	6	228.1752248	229.1830499	1.053049859
			OH	17	7	228.1878009	229.1956259	1.065625925
			2nd Tail					
			Possible Matches			Masses	Loss Seen	Difference
2nd Loss see	256.2565249		Link ID	Chain Length	Unsat			
Frag Mass	456.1534751	Data Location	Diol	17	2	254.2609659	255.2687909	0.987733954
		E1127	Amine	17	0	254.2847753	255.2926004	0.963924512
			OH	18	1	254.2973514	255.3051764	0.951348446
			Am+OH	17	7	255.138505	256.14633	0.110194869
			ET	18	7	255.1748905	256.1827155	0.073809361
			ES	16	0	255.2324054	256.2402305	0.016294425
			ET	17	0	255.2687909	256.276616	0.020091083
			Am+OH	17	7	256.1701395	257.1779645	0.92143961
			Diol	18	8	256.1827155	257.1905406	0.934015676
			Amine	18	6	256.206525	257.21435	0.957825118
			OH	19	7	256.219101	257.2269261	0.970401184
			Am+OH	16	0	256.2640399	257.2718649	1.015340054
			Diol	17	1	256.276616	257.284441	1.02791612

Figure 3.6 - Tail loss lookup interface for determining possible combinations of tail units on a given phospholipid. In this example PC 16:0/14:0 from Figure 3.4 is shown

Instrumental parameters as well as other sample preparation steps were optimized for the analysis of phospholipids by direct infusion mass spectrometry. The result is a method suitable for use on samples containing unknown composition and low concentrations of phospholipids while in the presence of organic contaminants. Furthermore, a method for the identification of the phospholipids by exact mass using neutral loss and precursor ion scan modes was developed and shown to be crucial in the identification of the lipids. Finally a method for the identification of the tail units present on the phospholipids was achieved by using product ion scanning mode and the mass of the fragment ions.

Chapter 4: Results

4.1 Calibration Standards

For the analysis and quantification of the phospholipids in the samples a variety of lipid standards were used to calibrate the response of the unknown lipids in the samples. Table 4.1 shows the standards used for the calibration and quantification of unknown lipids.

Phospholipid Class	Internal Standard	Recovery Standard	Calibration Standard
Phosphatidylethanolamine	PE 14:0	PE 8:0	PE 12:0 PE 16:0 PE 18:0 PE 18:0/18:1 PE 18:1
Phosphatidylcholine	PE 14:0/16:0	PC 12:0	PC 16:0 PC 18:0 PC 18:0/18:1 PC 18:1 PC 18:2 PC 20:0 PC 21:0 PC 16:0/18:1
Phosphatidylglycerol	PG 12:0	PG 17:0	PG 16:0 PG 18:0 PG 18:0/18:1 PG 18:1 PG 18:2
Phosphatidic acid	PA 10:0	PA 12:0	PA 18:0 PA 18:1 PA 18:2 PA 16:0 PA 16:0/18:1
Phosphatidylserine	N/A	PS 10:0	PS 14:0 PS 18:0 PS 18:1

Table 4.1 - Phospholipid standards used in the analysis of unknown lipid samples

The internal standard is added to all samples being run including both unknown samples and calibration samples. This is to insure that the instrument response does not vary substantially over the course of all samples. The internal standards being used have the potential to occur naturally in bacteria, however there is a preference for standards that typically do not occur in nature. This is not always possible and to confirm that a standard is not present in the sample, the samples are run without the presence of the internal standard to insure there is no overlap with a naturally occurring lipid in the sample. The concentrations of calibration standards being used range from approximately 10 nM up to 5μM giving the instrument a dynamic range of 2.5 orders of magnitude. The relative response of each of the standards is compared to the response of the internal standard averaged over all of the runs. These relationships are shown in Figures 1.1 and 1.2 for the positive mode phospholipids, PE and PC. The response factors are used when calculation the approximate concentration of the unknown phospholipids in the samples.

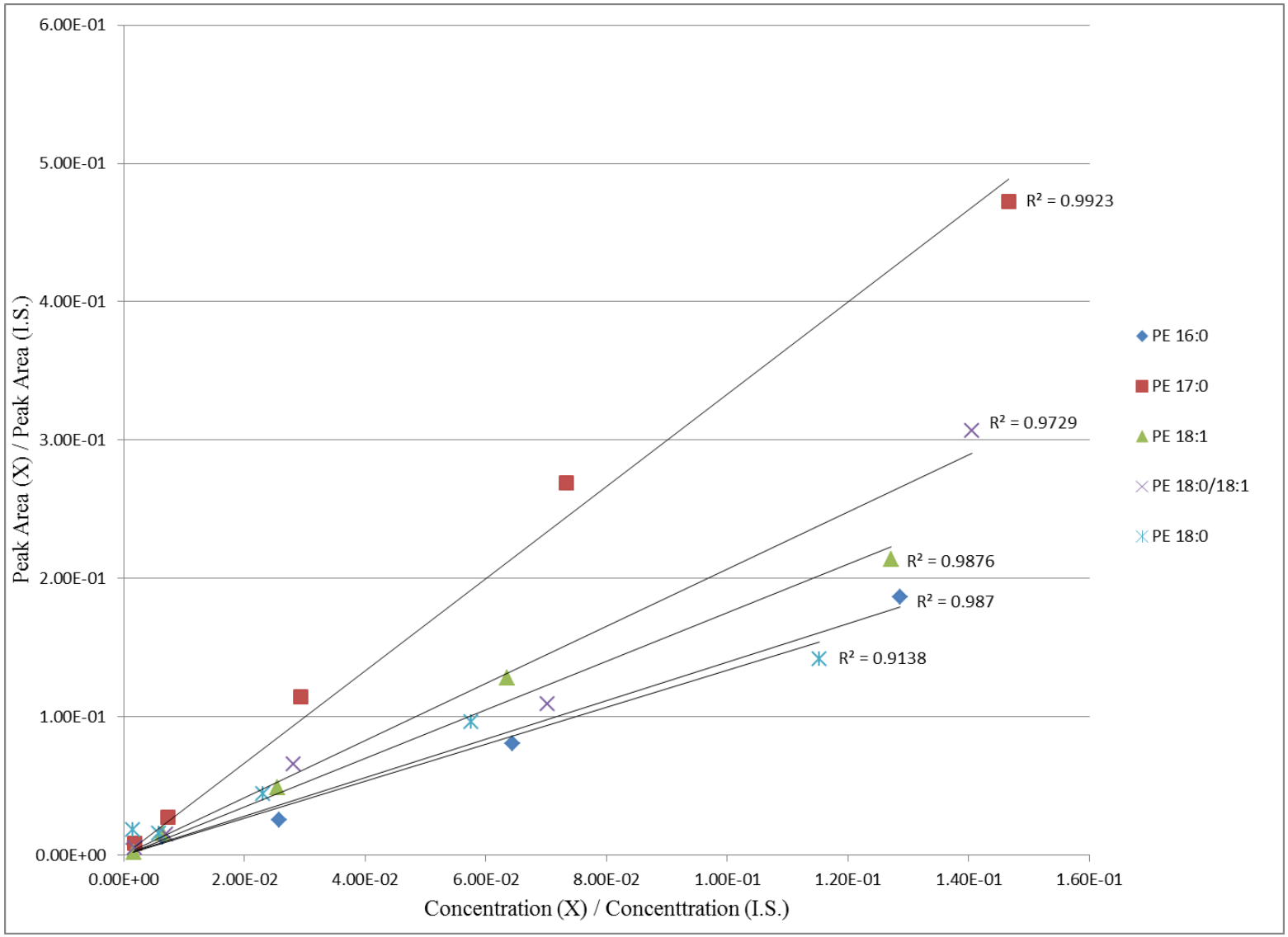

Figure 4.1 - Relative response of PE standards compared to the internal standard PE 14:0

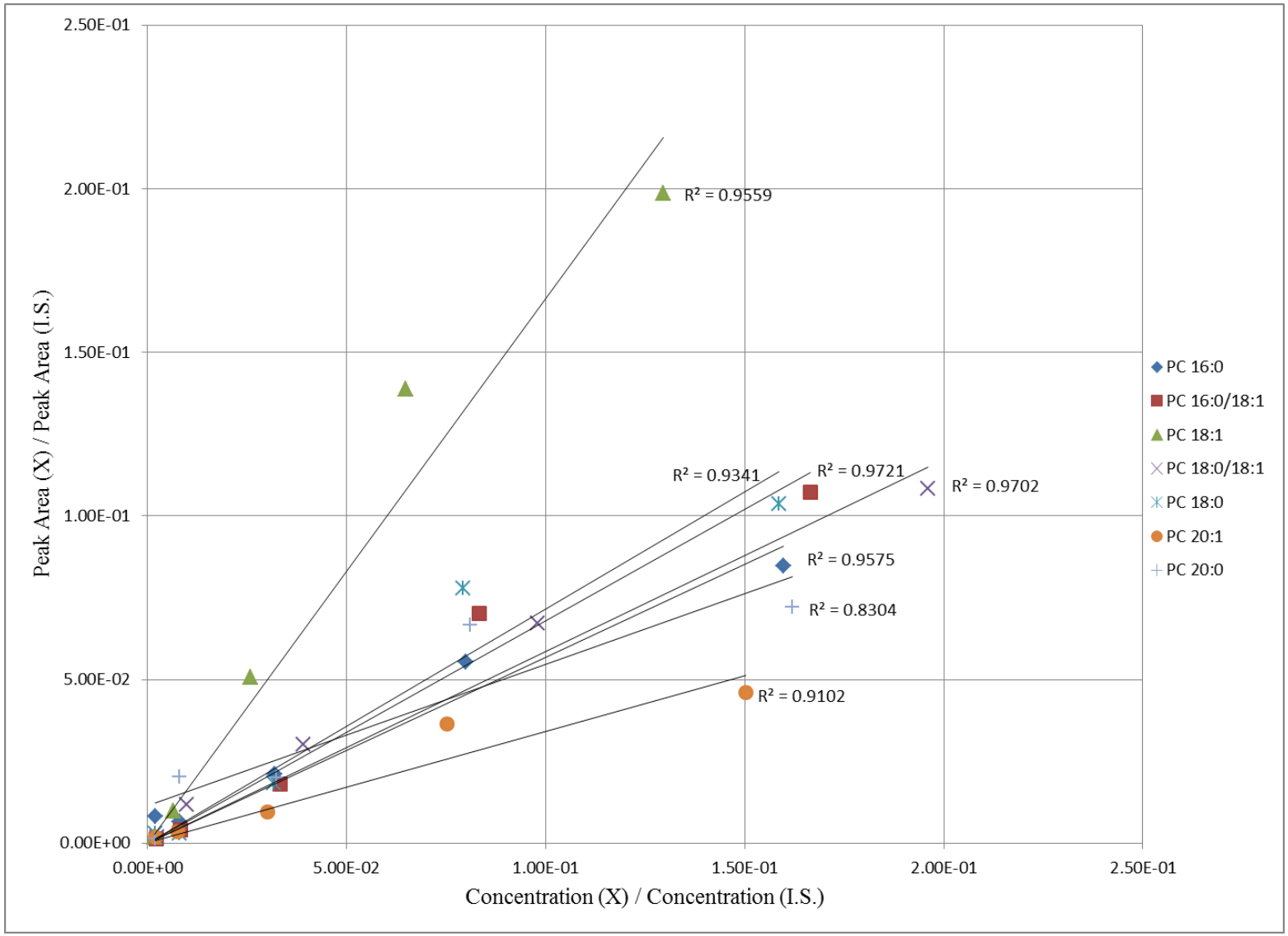

Figure 4.2 - Relative response of PE standards compared to the internal standard PC 16:0/14:0

4.2 Syncrude Composite Tailings Well Water Samples

Composite tailings samples were collected by the Dr. Warren group according to the protocols outlined in section 2.7. A total of fifteen samples were collected and analyzed including four well across a one year period and a process water sample from the beginning of the study period. Each sample was extracted and analyzed by mass spectrometry in triplicate with the goal of determining whether trends exist between samples.

Figure 4.3 shows a typical mass spectrum of the extracted water samples. The spectrum of the neutral loss of 147 is for the PE lipids and the neutral loss of 189 is for the PC lipids. The peaks at 642 and 455 in the PE spectrum correspond to the internal standard and the recovery standard respectively. The peak at 712 and 628 in the PC spectrum correspond to the internal standard and recovery standard. All other signals correspond to potential phospholipids. As previously discussed one of the methods employed in the verification of real signals is to look at the pattern between the two spectrum, the mass difference between a PE and its complimentary PC is 42 mass units, by shifting the spectrum of the PEs by +42 it is possible to line the two spectrums up to determine the complimentary lipid pairs and further confirm their presence in the sample. Figure 4.4 shows the shifted spectrum of PE and the original PC spectrum to show this relationship. This shifted spectrum shows that a number of fatty acid tails are common across the two phospholipid classes strengthening the argument that patterns arise where an organism will utilize the same fatty acids across different phospholipid classes.

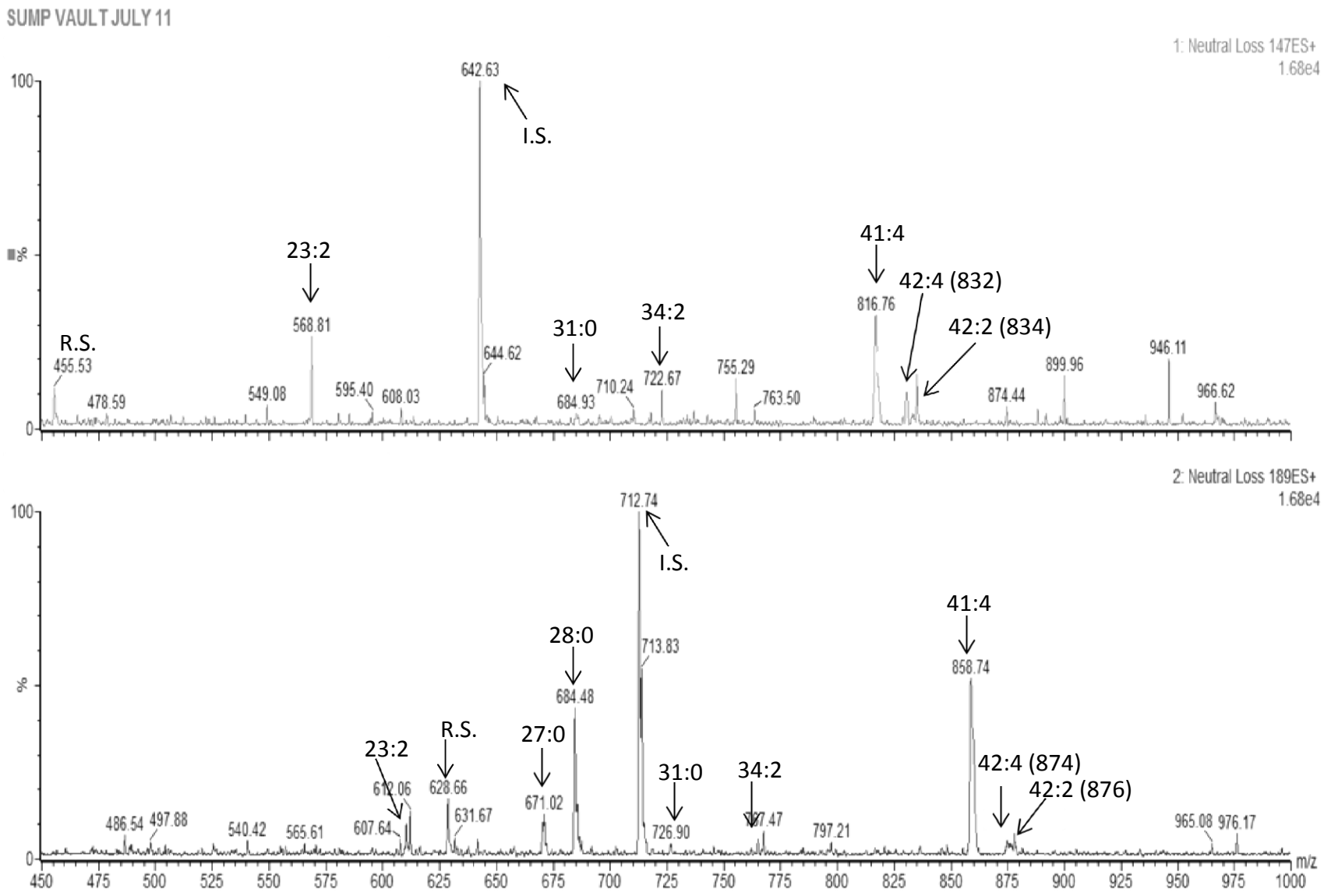

Figure 4.3 - Phosphatidylcholine (PC) and phosphatidylethanolamine (PE) profiles in the Sump Vault July 2011

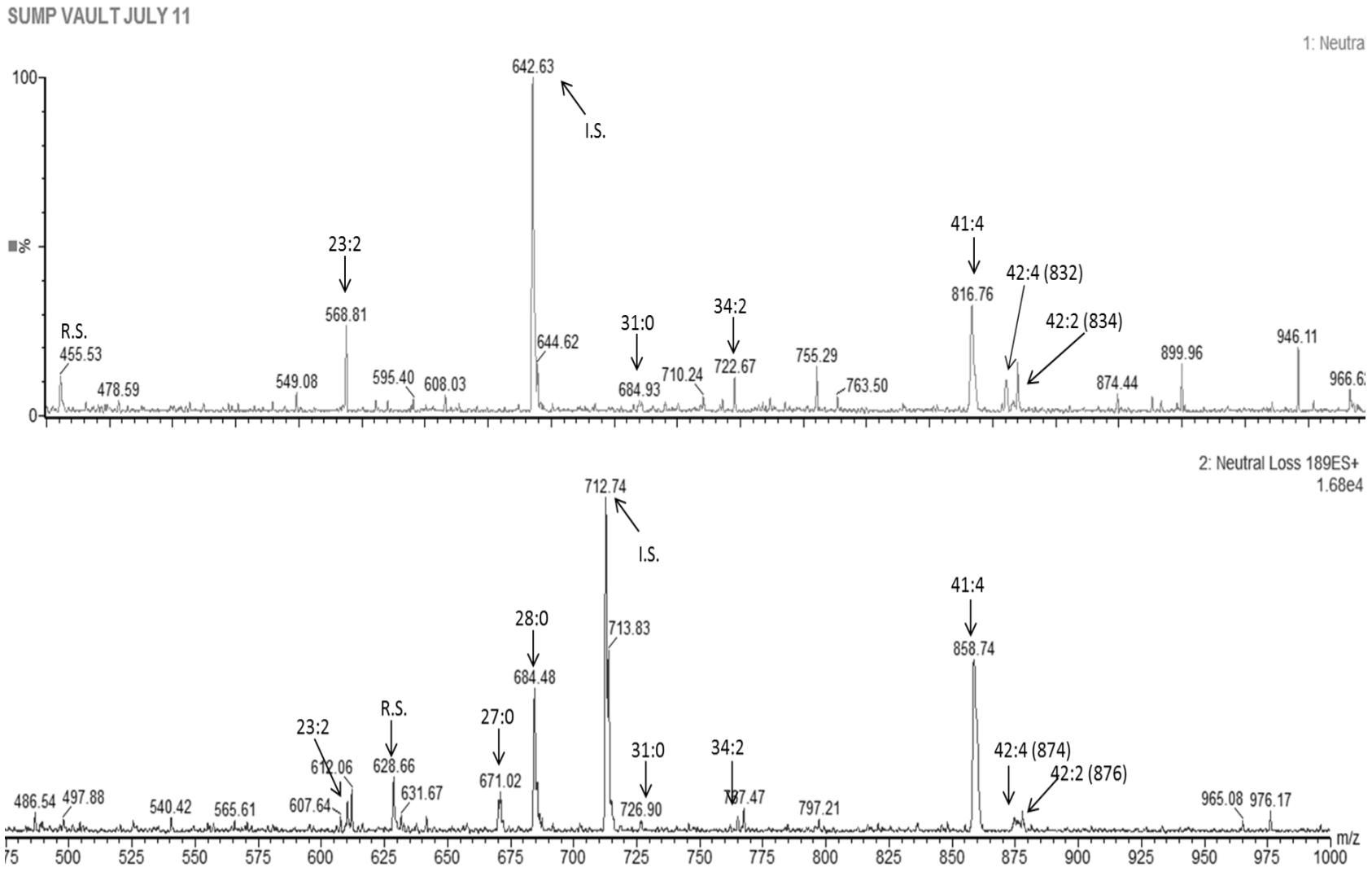

Figure 4.4 - Phosphatidylcholine (PC) and phosphatidylethanolamine (PE) profiles in the Sump Vault July 2011 with an +42m/z offset applied to the PE spectrum

The peak area data from each of the mass spectrum of the unknown samples was then analyzed to develop a list of potential phospholipids in the given sample. Table 4.2 shows the number of unknown phospholipids found in each sample with the total approximated concentration of phospholipid found in the sample.

Sample	Total Number of Phospholipids	Total Concentration of phospholipid in sample* (nM)
Process Water (July 2011)	18	250
Sump Vault (July 2011)	31	750
Well 5d (July 2011)	21	500
Well 6a (July 2011)	17	250
Well 8c (July 2011)	18	250
Sump Vault (Feb 2012)	46	200
Well 6a (Feb 2012)	11	100
Sump Vault (May 2012)	31	200
Well 5d (May 2012)	33	150
Well 6a (May 2012)	14	375
Well 8c (May 2012)	16	150
Sump Vault (Aug 2012)	30	500
Well 6a (Aug 2012)	16	250
Well 8c (Aug 2012)	16	375
Sump Vault (Oct 2012)	29	175

Table 4.2 - Number of unknown phospholipids and approximate total concentration in samples
*concentration is only approximate because of variation in relative response factors and limited number of standards available

To look further into changes occurring in the phospholipids present within the samples, multivariate analysis was performed using the SIMCA-P software. Figure 4.6 shows the principal component analysis (PCA) of all five wells across all time points. The $R^2X$of the data was 0.815, implying a large amount of the data was included in the principal component, and the Q^2 was 0.284 suggesting that there were no obvious differences from one sample to the next.

Figure 4.5 shows the loading plot for the PCA plot of all data points. It shows how the PCA locations are derived and which phospholipids are responsible for shifts in the corresponding direction.

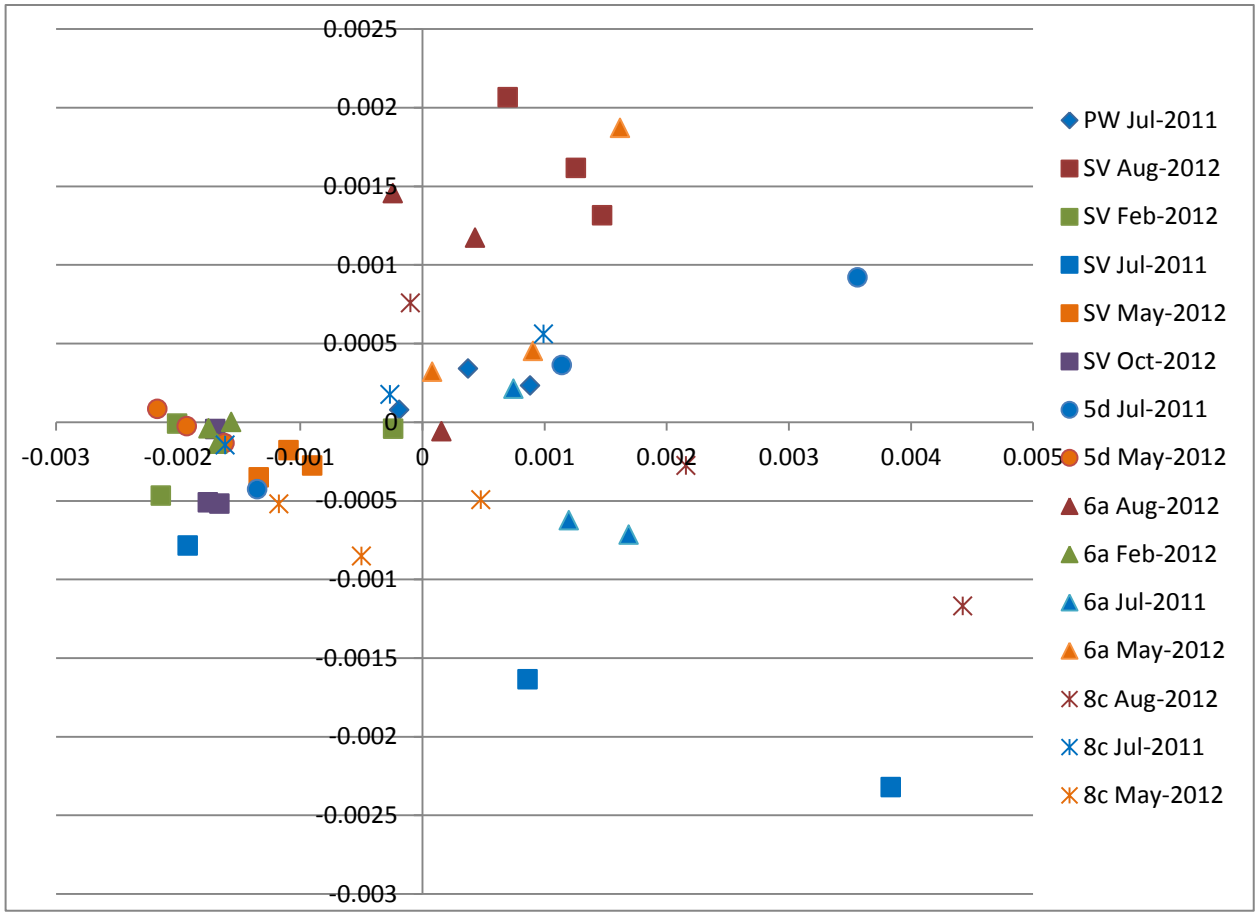

Figure 4.6 - Principal Component Analysis of all well samples over all time points

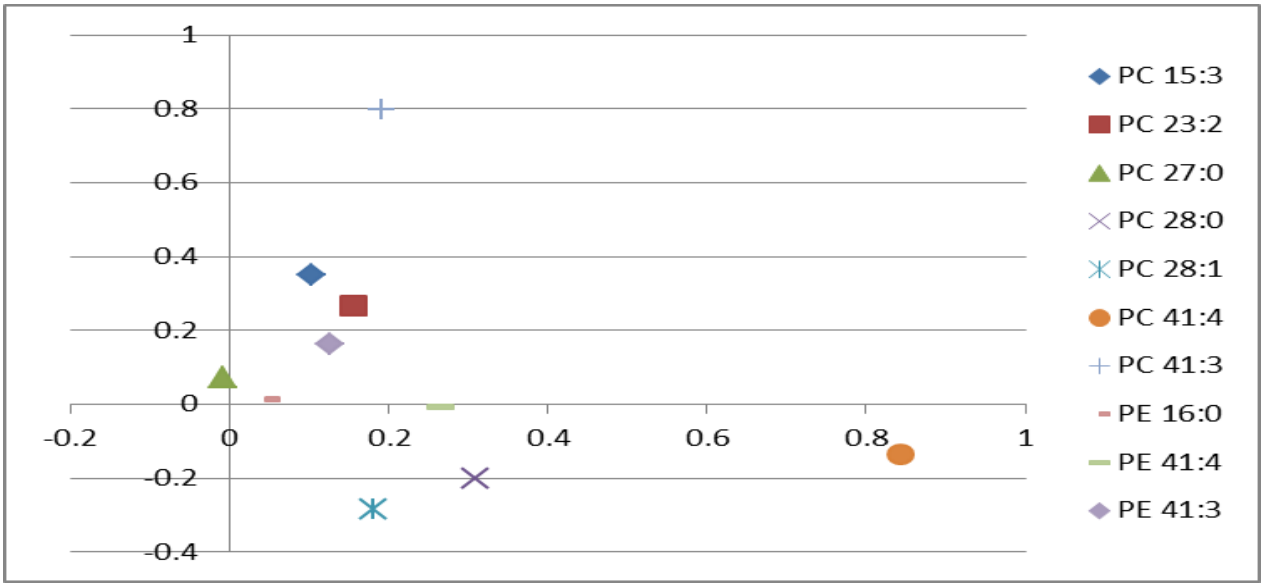

Figure 4.5 - Loadings plot for the PCA plot of all well samples

Figure 4.8 shows the OPLS-DA of well 6a over the course of a one year period. The R^2X value was 0.956, the R^2Y value was 0.759 and the Q^2 value was 0.675. This implies a large amount of the data makes up the components and with a Q^2 value of 0.675 a moderate fit and a reasonable difference in phospholipid profiles separating the different time points. Within the figure, the ovals represent the groupings of each triplicate analysis of the sampling dates.

Figure 4.7 shows the S-Plot for the OPLS-DA plot of well 6a over the course of the one year period. The S-Plot shows the relative importance of each phospholipid in representing the differences within the sample set.

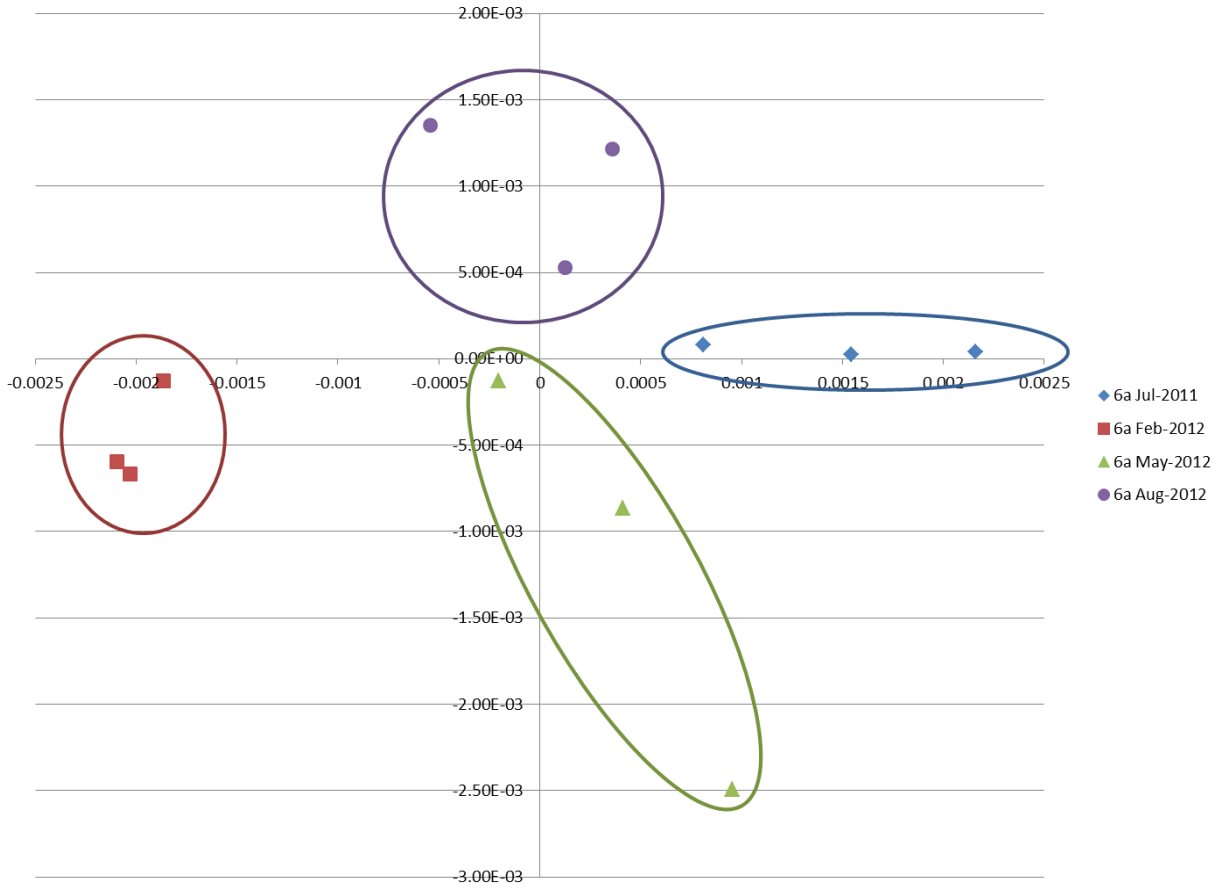

Figure 4.8 - OPLS-DA plot of Well 6a over four time points

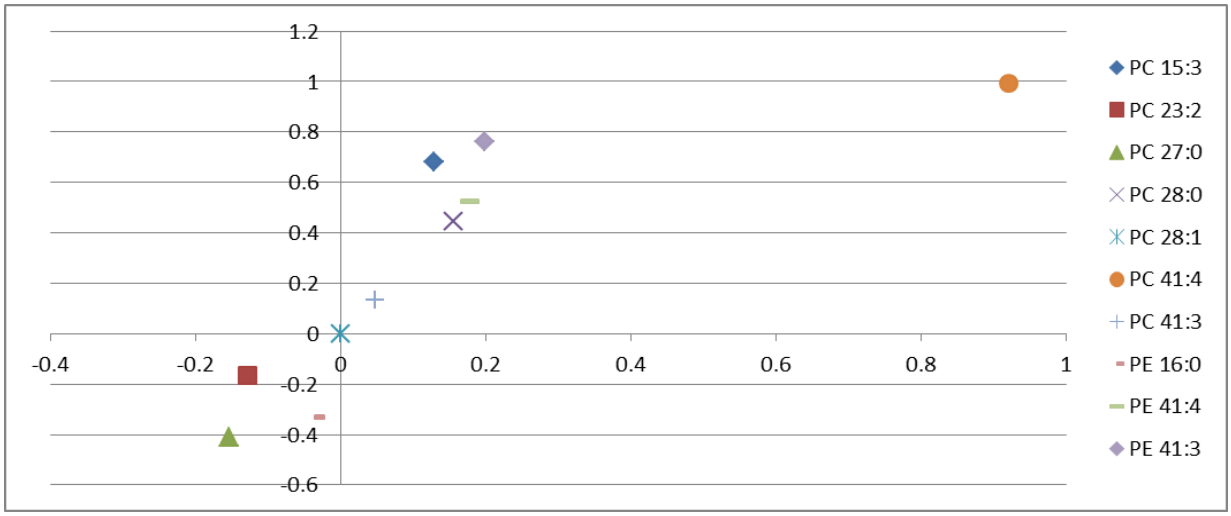

Figure 4.7 - S-Plot for the OPLS-DA plot of Well 6A over four time points

Figure 4.10 shows the OPLS-DA plot of the Sump Vault over the course of a one year period. The R^2X value is 0.985, the R^2Y value is 0.674 and the Q^2 value is 0.298 when considering all time points as separate groups. When considering July, August separate and February, October and May together the Q^2 becomes 0.723. This suggests that although trends correlating month to month changes are weak, seasonal trends are noticeably apparent. Within the figure, the light blue oval on the top right shows the grouping of Aug-2012 samples, the dark blue oval on the left shows the grouping of the colder months, Feb-2012, May-2012, and Oct-2012, and finally the red oval at the bottom shows the grouping of July-2011.

Figure 4.9 shows the S-Plot for the OPLS-DA plot of the sump vault samples over the course of the one year period. It represents the relative importance for each phospholipid in determining the differences between samples.

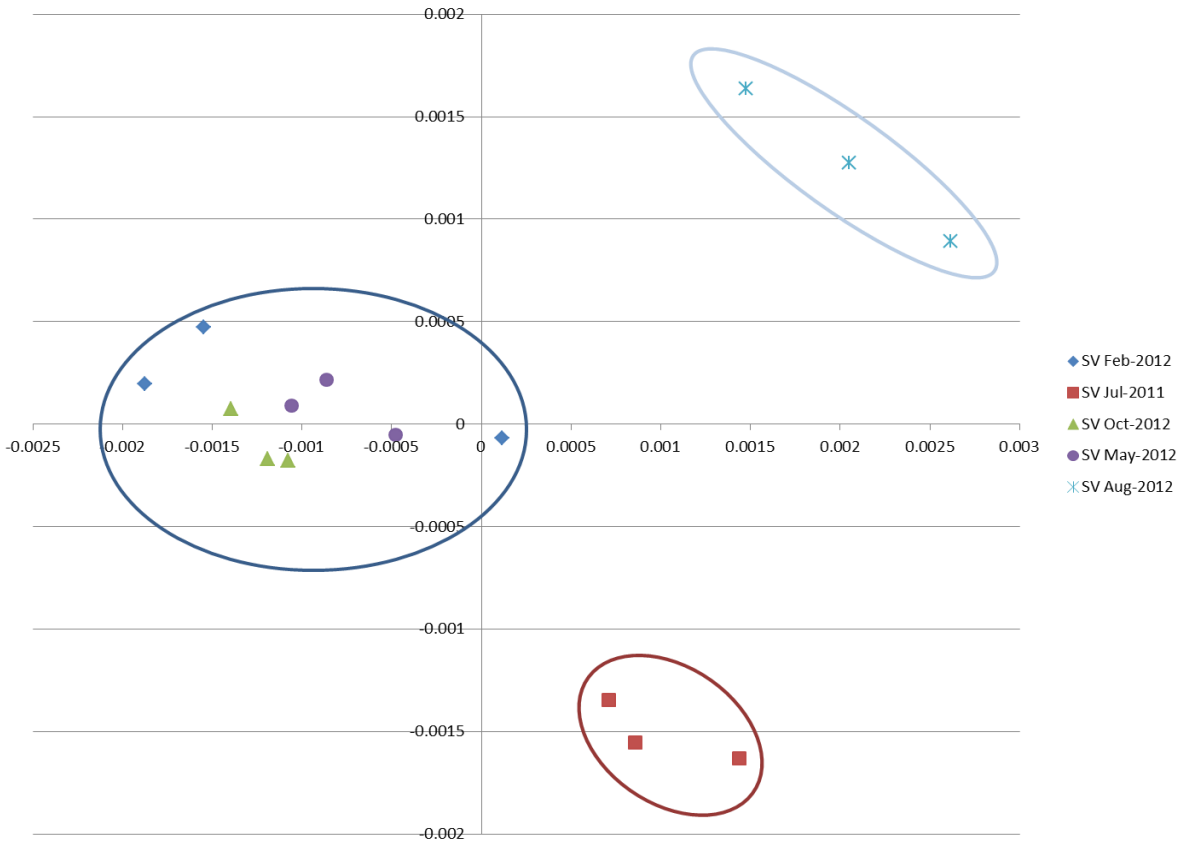

Figure 4.10 - OPLS-DA plot of the Sump Vault over an 11 month span showing seasonal differentiation

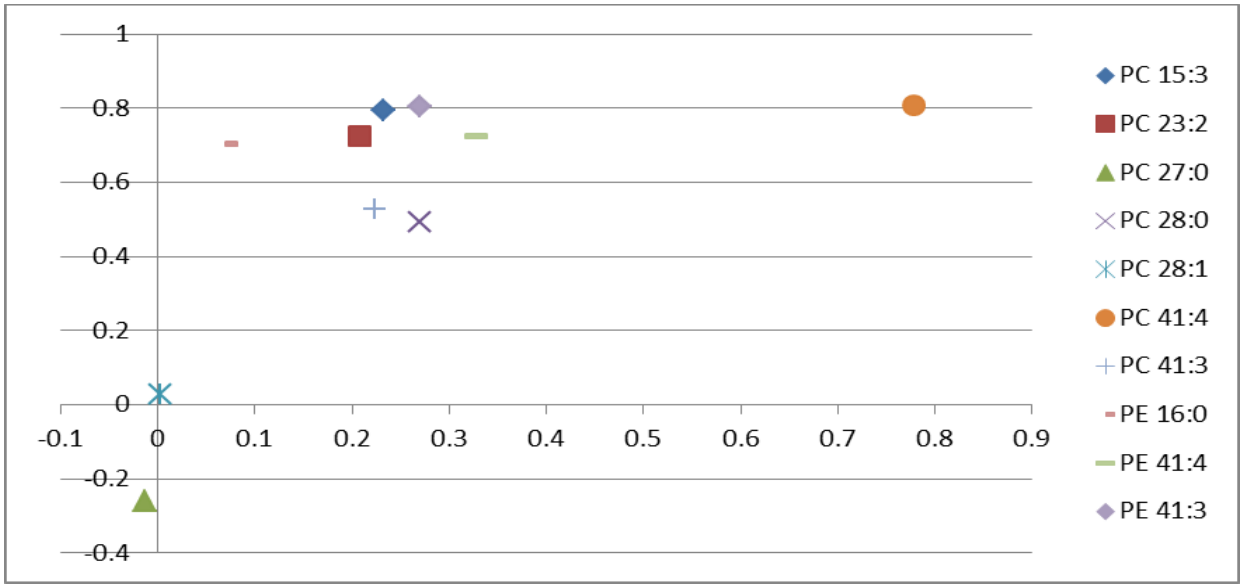

Figure 4.9 - S-Plot for the OPLS-DA plot of the Sump Vault samples

Figure 4.12 shows the OPLS-DA plot of Well 8c over the course of a one year period with three time samples. The R^2X value is 0.996, the R^2Y value is 0.598, and the Q^2 value is 0.714. This suggests a strong trend separating the different time points based on phospholipid profiles. Within the figure, the ovals show the groupings of the separate sampling dates.

Figure 4.11 shows the S-Plot for the OPLS-DA plot of the well 8c samples over the course of the one year period. The S-Plot shows the relative importance of each phospholipid with respect to the differences observed for each sample.

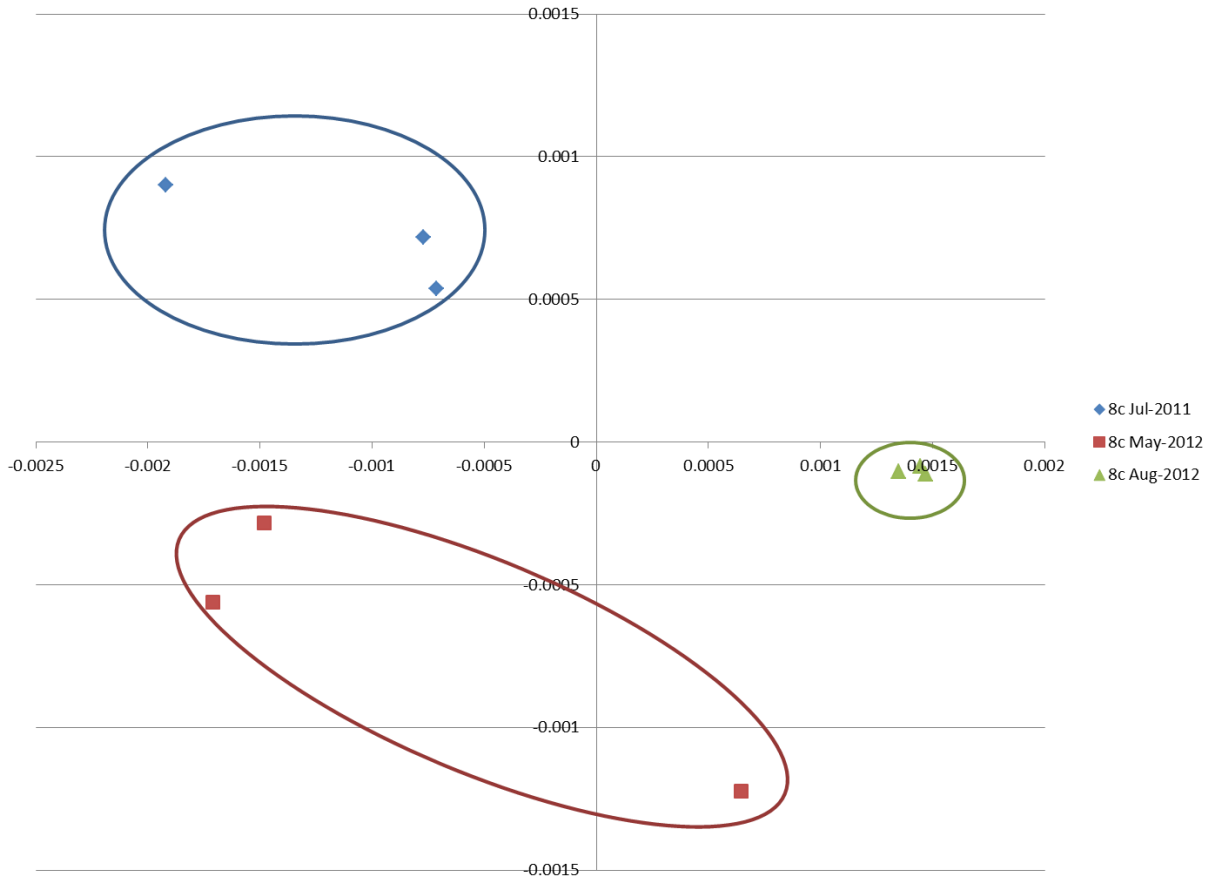

Figure 4.12 - OPLS-DA plot of Well 8c showing 3 time points over a one year period

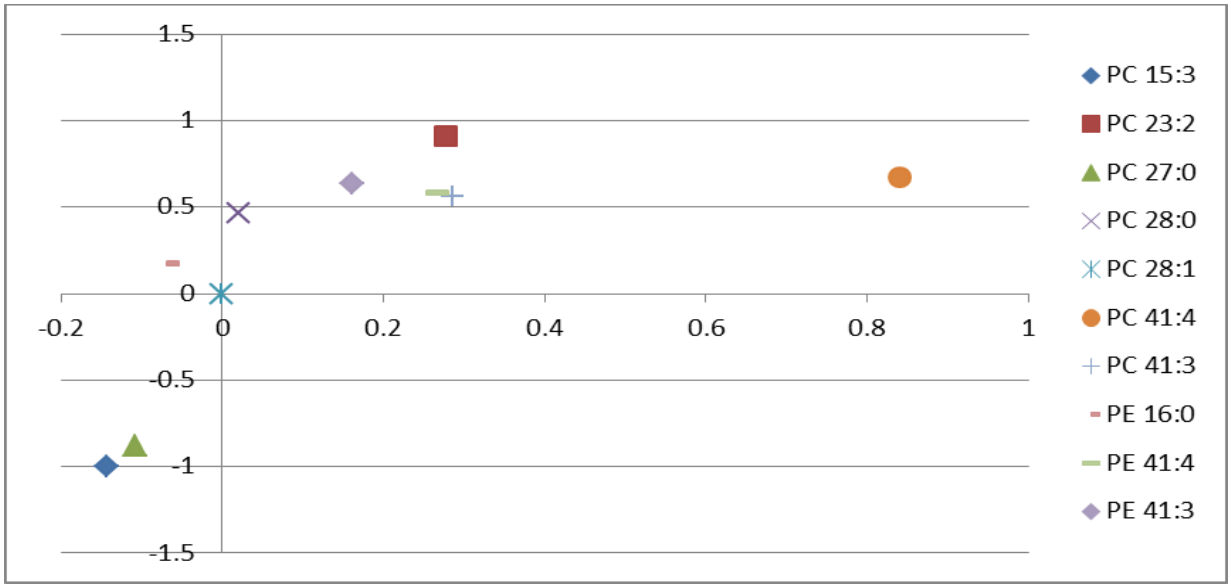

Figure 4.11 - S-Plot for the OPLS-DA plot of the Well 8c samples

Figure 4.14 shows the OPLS-DA plot of all samples taken during July 2011; this includes Well 5d, Well 6a, Well 8c, the Sump Vault and the Process Water. The R^2X value is 0.852, the R^2Y value is 0.199, and the Q^2 value is -0.109. This suggests that there is no difference in the phospholipid profiles between the different wells during the month of July.

Figure 4.15 shows the S-Plot for the OPLS-DA plot of all July 2011 samples. It represents the importance of each phospholipid with respect to the observed changes occurring with the samples.

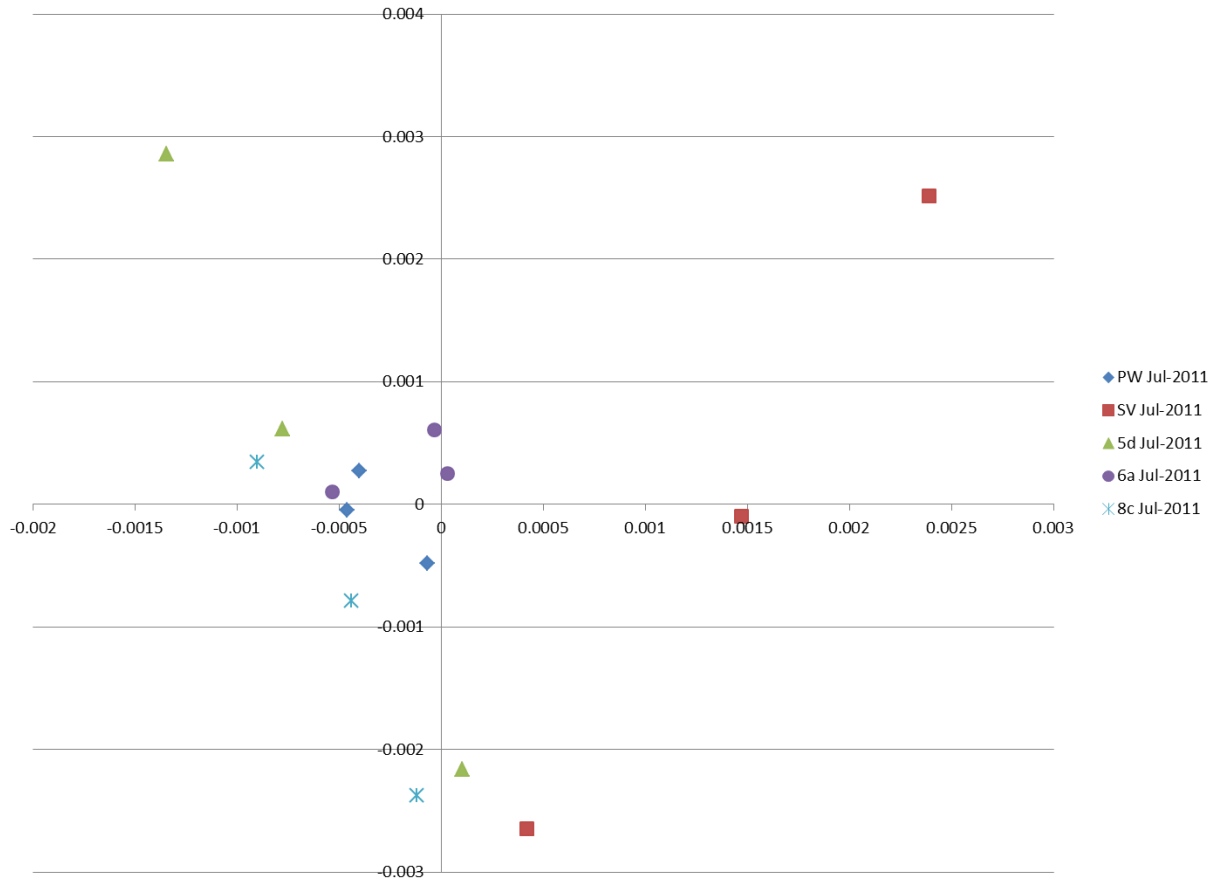

Figure 4.14 - OPLS-DA plot for all well samples from July 2011

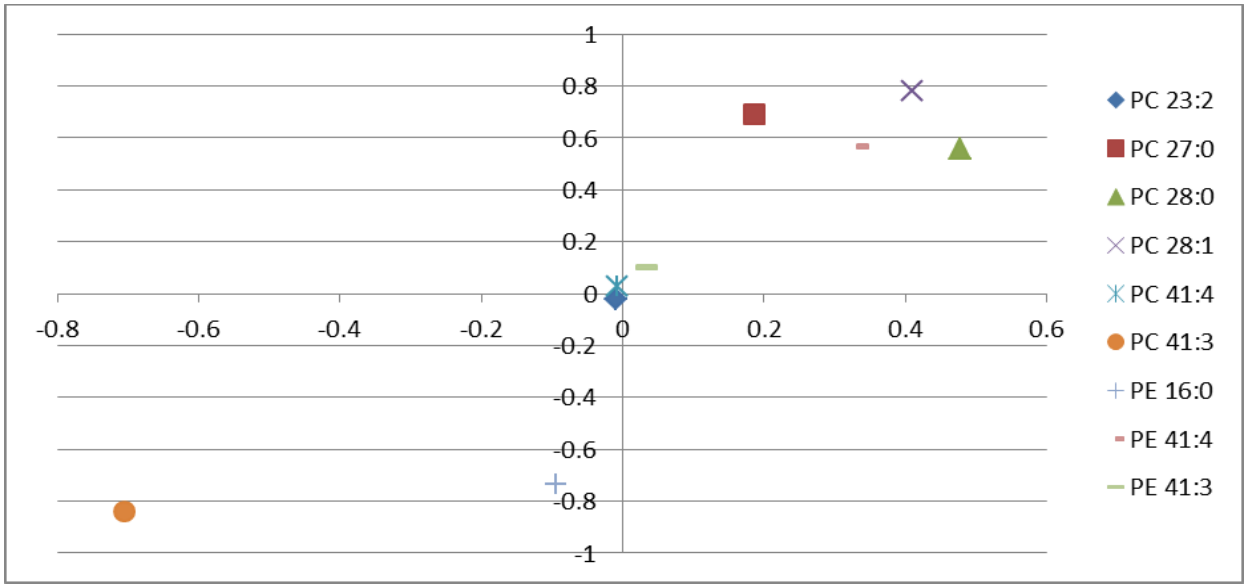

Figure 4.13 - S-Plot for the OPLS-DA plot of the July 2011 samples

Figure 4.16 shows the OPLS-DA plot of all samples taken during May 2012; this includes Well 5d, Well 6a, Well 8c, and the Sump Vault. The R^2X value is 0.940, the R^2Y value is 0.772, and the Q^2 value is 0.641. This suggests a moderate trend showing differences between the phospholipid profiles for the different wells during the month of May. Within the figure the ovals represent the groupings of the individual months.

Figure 4.15 shows the S-Plot for the OPLS-DA plot of all of the May 2012 samples. It represents the importance of each phospholipid with respect to the observed differences for the May 2012 samples.

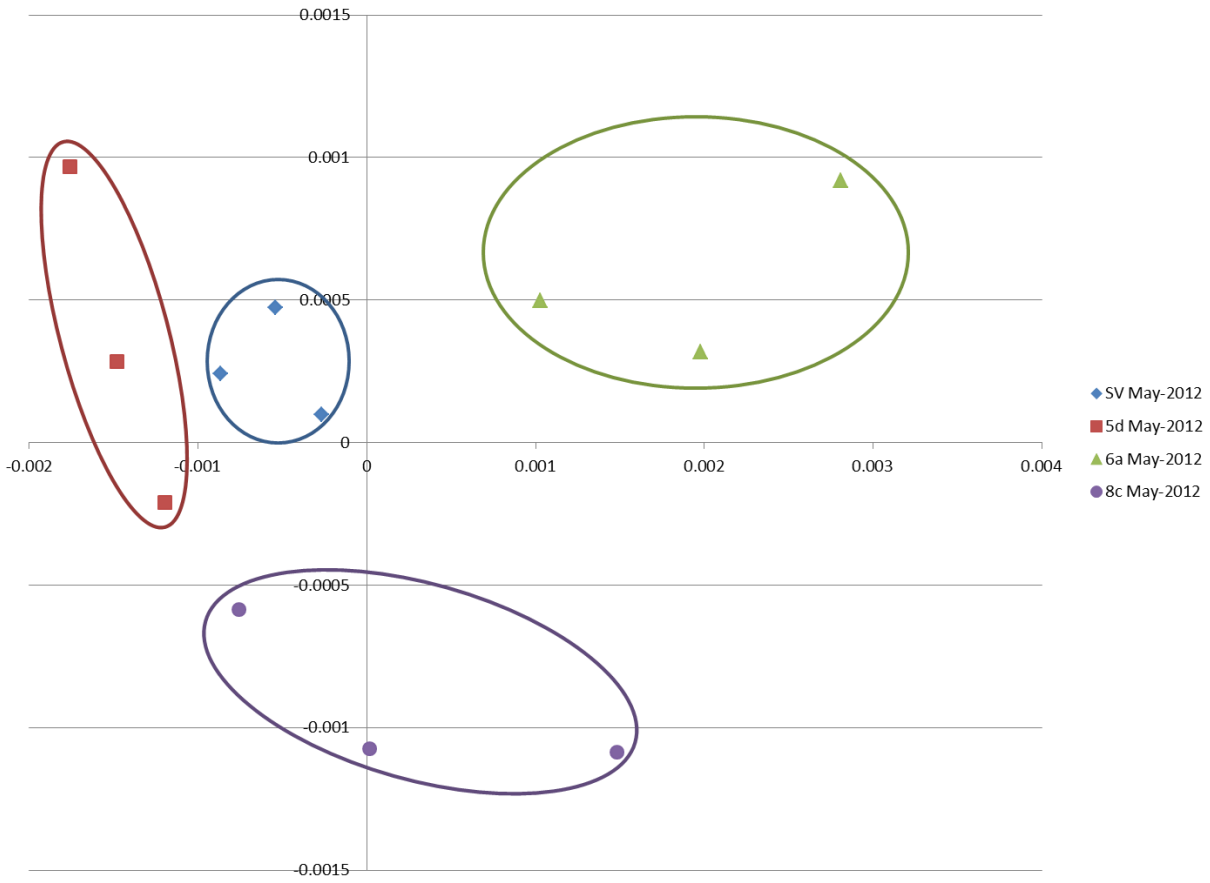

Figure 4.16 - OPLS-DA plot showing a moderate trend between four of the wells during the May 2012 sampling period

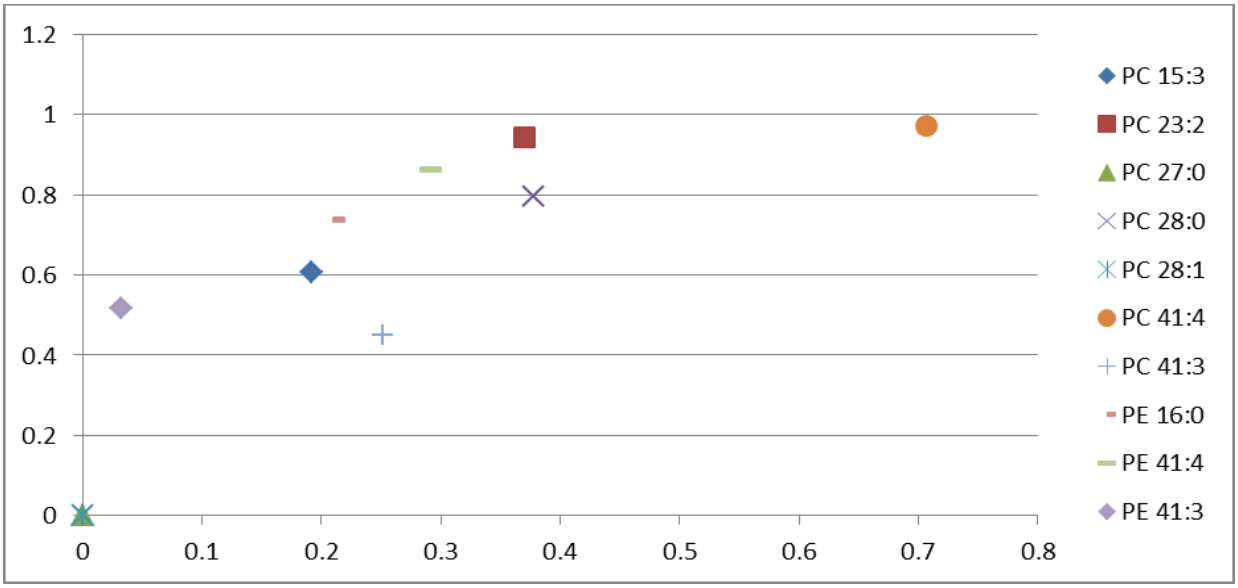

Figure 4.15 - S-Plot for the OPLS-DA plot of the May 2012 samples

Figure 4.18 shows the OPLS-DA plot of all samples when grouped as month of sampling. The r^2x value is 0.91, the r^2y value is 0.232, and the q^2 value is 0.114. This suggests little to no differences exist when comparing the phospholipid profiles for all water sample data points across all times.

Figure 4.17 shows the S-Plot for the OPLS-DA plot for all the well water samples taken over the one year period. It should the importance of each of the phospholipids with respect to any differences seen within all the well water samples.

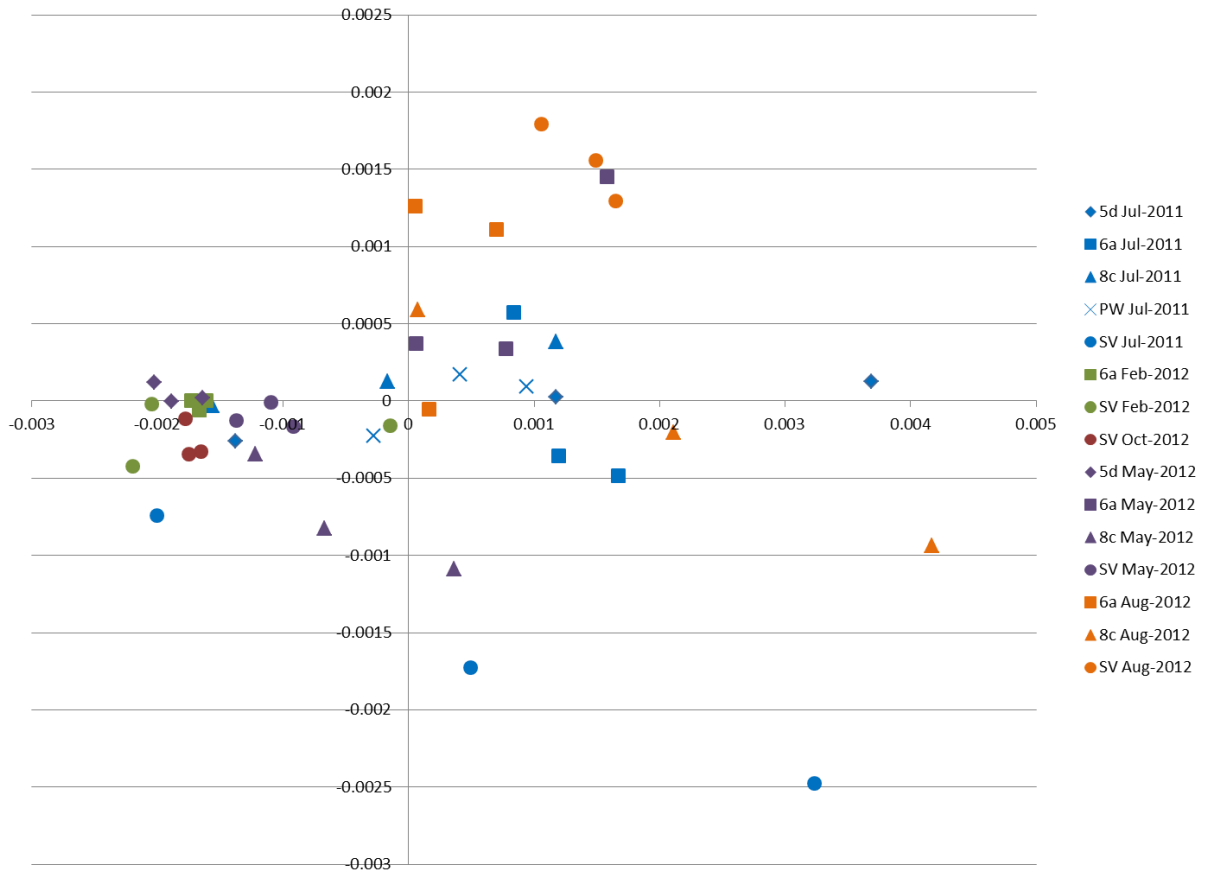

Figure 4.18 - OPLS-DA plot of all samples showing no trends

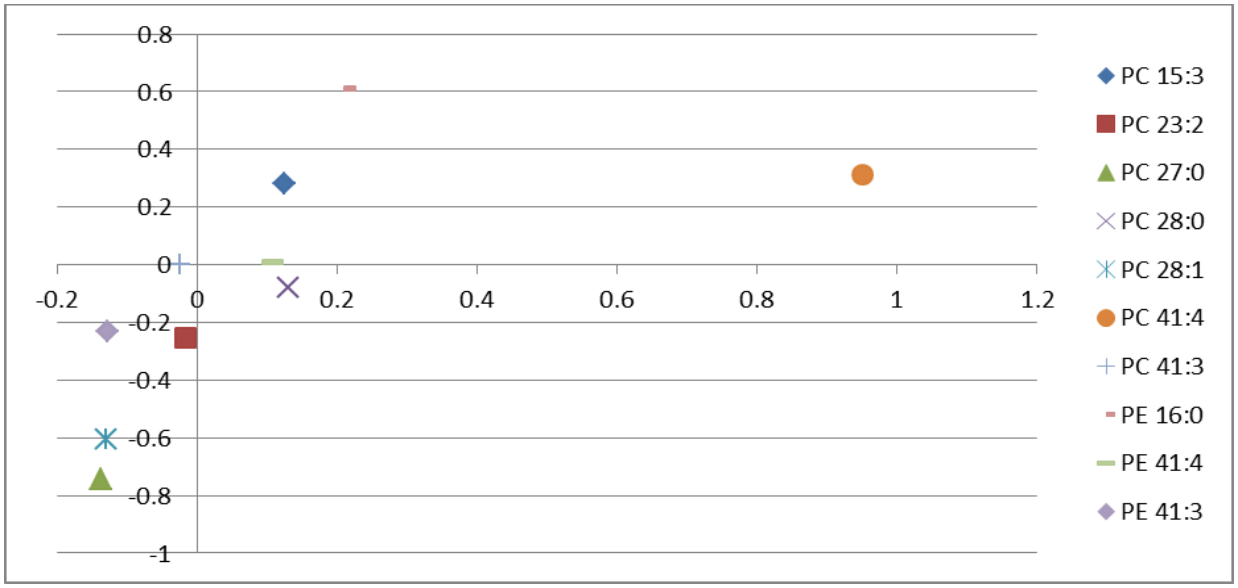

Figure 4.17 - S-Plot for the OPLS-DA plot of all the water samples

Figure 4.20 shows the OPLS-DA plot of all samples when grouped as seasons, with samples taken in July and August grouped together and October, February and May grouped together. The r^2x value is 0.79, the r^2y value is 0.504 and the q^2 value is 0.433. This suggests that minor phospholipid profile differences exist when comparing the summer months to the rest of the year.

Figure 4.19 shows the S-Plot for the OPLS-DA plot of all samples when grouped by season. It represents the importance of each phospholipid with respect to the changes in phospholipid profiles observed.

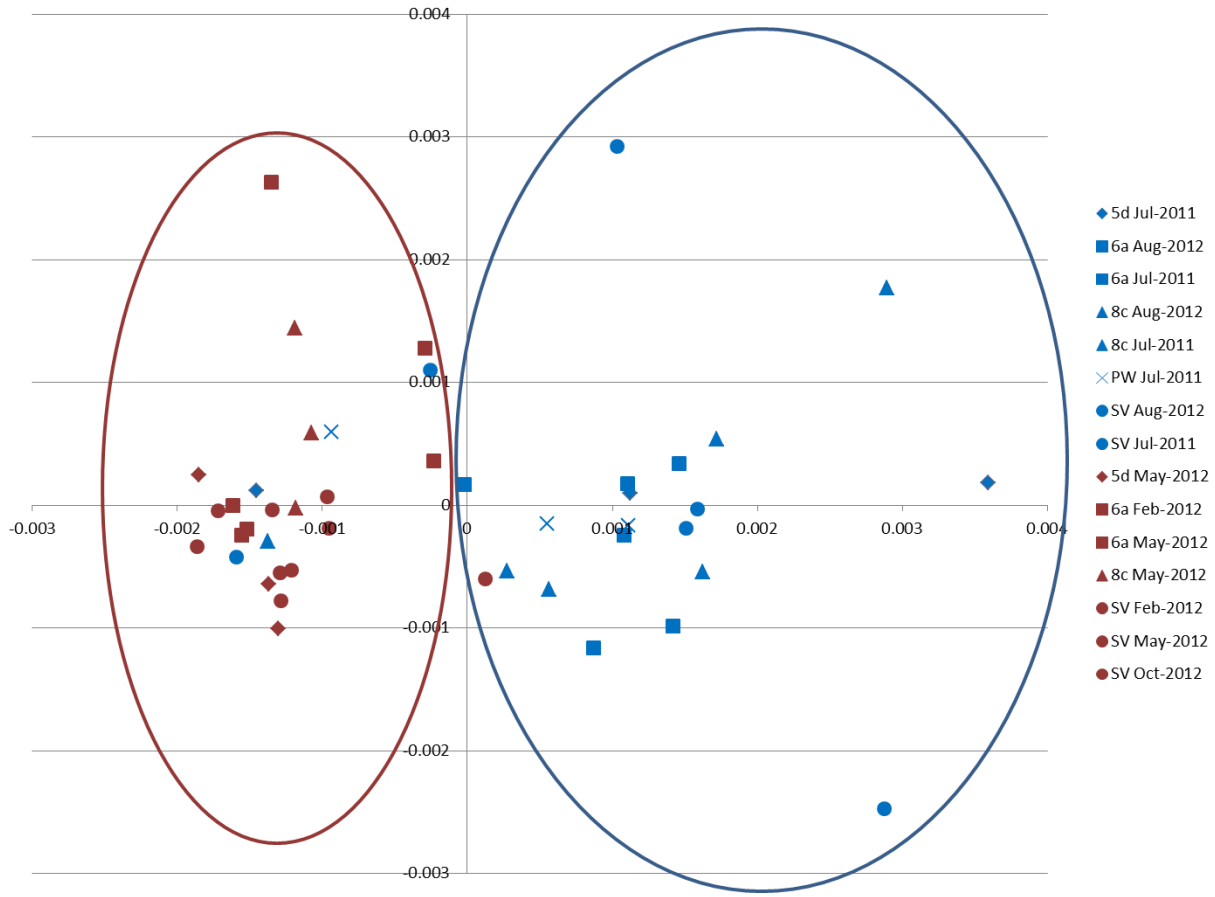

Figure 4.20 - OPLS-DA plot showing a moderate trend between summer months versus the rest of the year

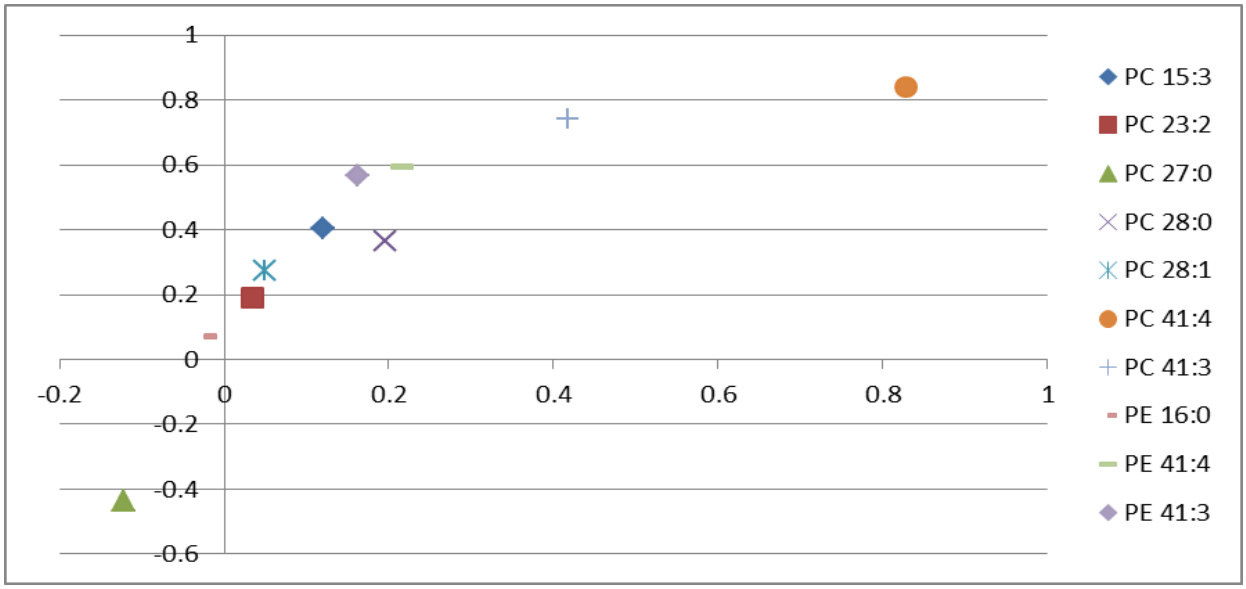

Figure 4.20 - S-Plot for the OPLS-DA plot showing the summer months vs the rest of the samples

4.3 Syncrude Composite Tailings Well Sediment Samples

A modified Blight and Dyer method for the extraction of phospholipids was applied to the sediment samples collected by the Dr. Warren group as outlined in section 2.9. The initial goal was to develop the method to be able to reproducibly determine the phospholipid profile of the sediment samples; however the main drawback of the direct-infusion method becomes quite apparent when dealing samples of this type. Figure 4.13 shows the mass spectrum of the Well 6a sediment sample collected July 2011; noticeably, the total signal intensity of this spectrum is quite low when compared to the spectrums of well water samples. This is largely due to the high concentration of other organic materials present in the sediment, through the bitumen extraction process not all bitumen is extracted leaving relatively large quantities of organics in the sediment. The Blight and Dyer extraction methods does compensate for this by incorporating purification steps including a silica column. The sample is concentrated after the silica column, the resulting solution is still coloured and has a yellow-orange tint to it, and this is a good indicator that there is still a significant amount of organic material remaining. This organic material caused significant ion suppression, when comparing the signal intensity of the unsuppressed internal standard to that of the suppressed the decrease in signal was circa one order of magnitude.

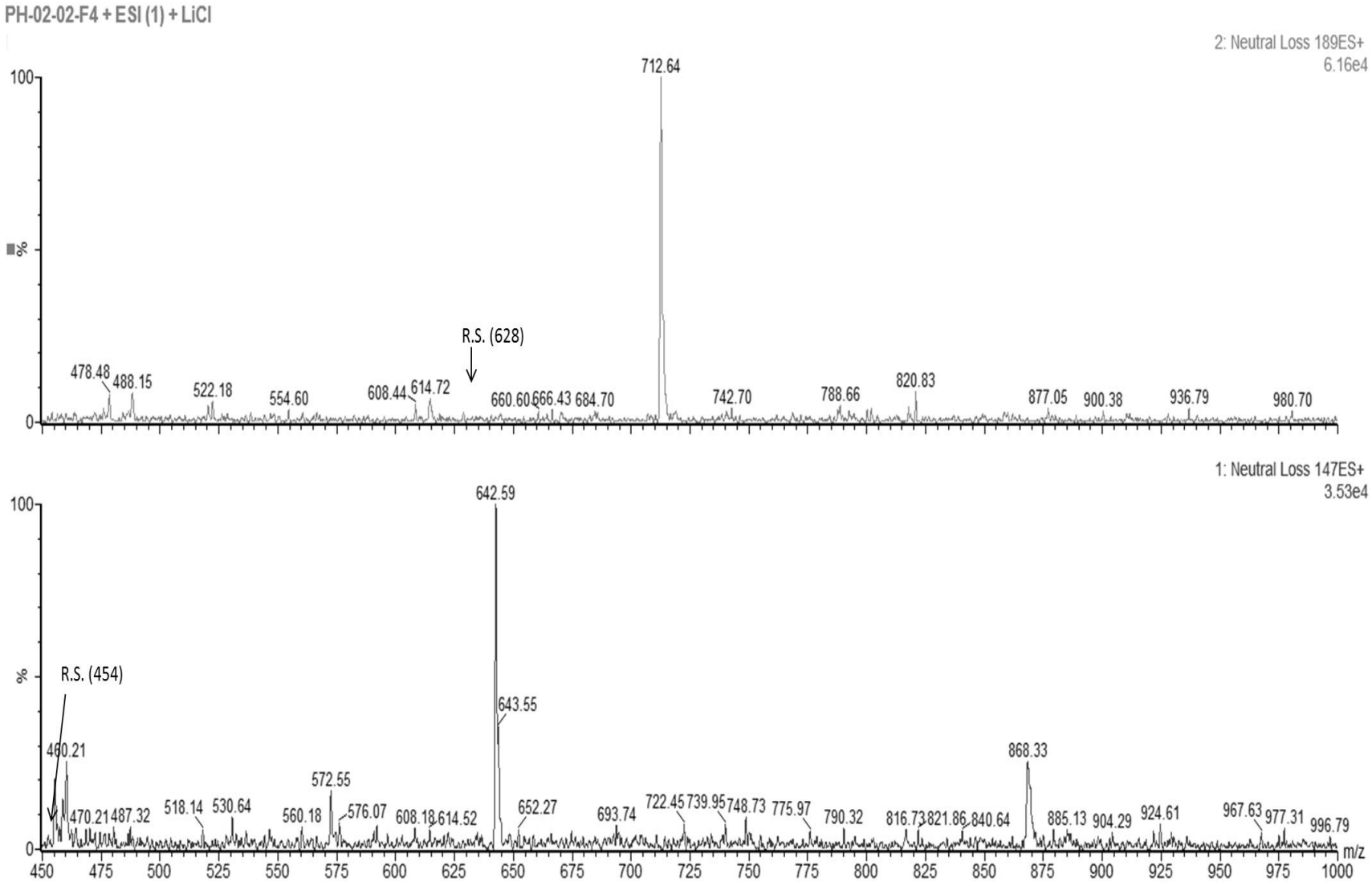

Figure 4.21 - Mass spectrum of the Well 6a soil sample July 2011 showing large amount of ion suppression and lack of recovery

Chapter 5: Discussion

5.1 Calibration Standards

The purpose of using a spiked internal standard is to insure that the instrument continues to respond in the same manor throughout the entire experiment; an additional advantage to using an internal standard is that it may be used to compensate for injection errors and it serves as a basis for data normalization. Figure 5.1 shows the consistency of the internal standard across the calibration curve injections. The percentage of variance for the PE 14:0 standard is 16% and for PC 16:0/14:0 is 14%. This allows the internal standards used in the unknown samples to be compared with the average peak intensity of the same internal standard mix in the calibration

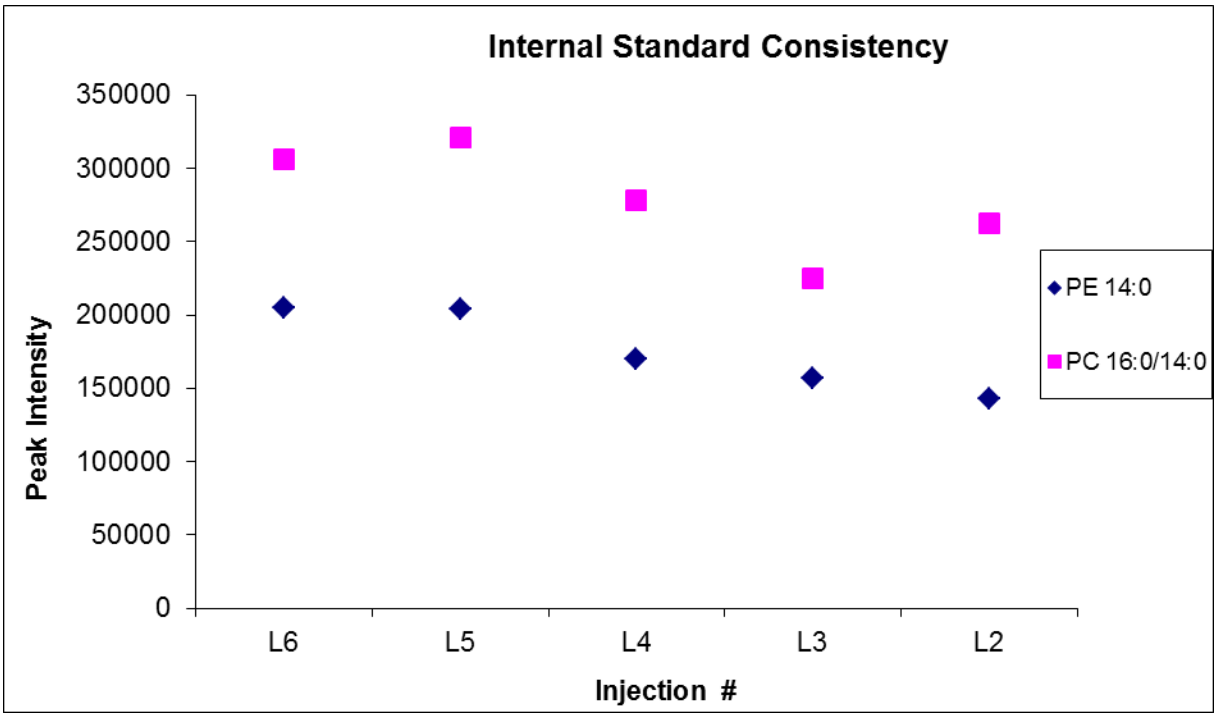

Figure 5.1 - Internal standard consistency across multiple injections

standard injections. This would be repeated each time a new set of calibration standards are run or every seven unknown sample injections.

The drift in instrumental response can cause statistically significant changes in response from the beginning of a series of experiments to the end. The responses of the recovery standards are observed at three points during the series of experiments to insure that this is not the case. The recovery standards are observed prior to the calibration standards, then again following the calibration standards and finally after all unknown samples. Figure XX shows the response of the PE 8:0/8:0 and PC 12:0/12:0 recovery standards. Their percentage variations were 17.0% and 7.2% respectively. The internal standards used in each of these runs, PE 14:0/14:0 and PC 14:0/16:0, were also compared and their percentage variations were 7.7% and 9.2% respectively.

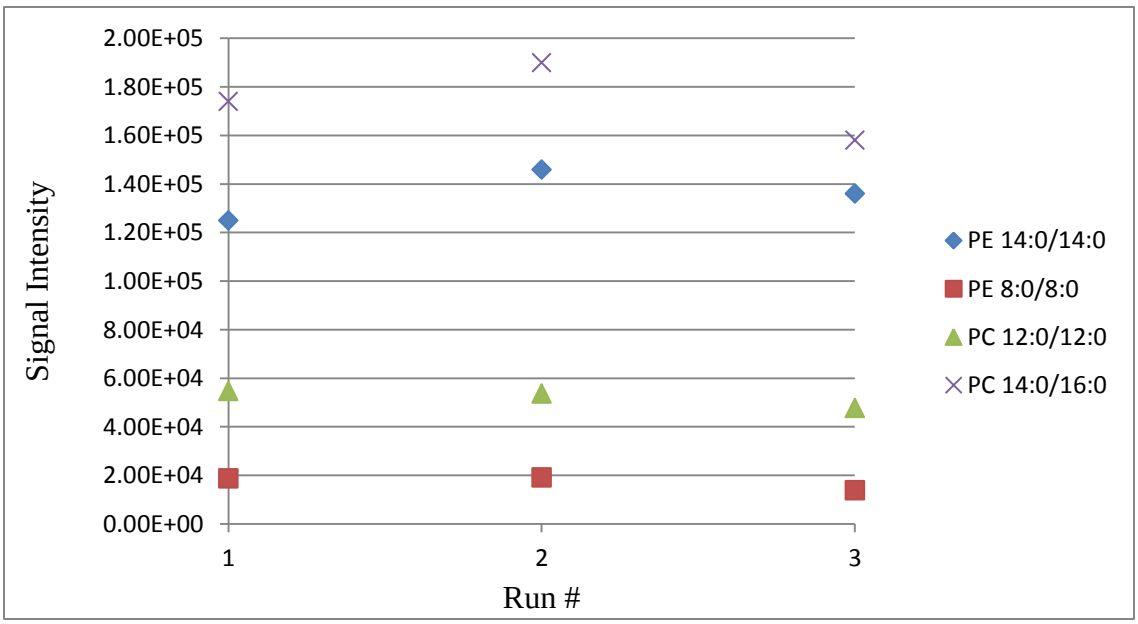

The relative response factor is a measure of peak area of one standard in relation to the internal standard signal. Table 5.1 shows the relative response factors for the PE and PC calibration standards in relation to their respective internal standard. Typically, these response factors are used to compare unknown concentrations in samples to the internal standard in order to determine the concentration of the phospholipid in the sample. In this project, an approximate concentration of unknown lipids is determined by using the average relative response factor for each phospholipid class. It should be noted that although this method is convenient it only provides a concentration accurate to +/- 50%.

Calibration Standard	Relative Response Factor
PE 16:0/16:0	1.67
PE 17:0/17:0	4.00
PE 18:1/18:1	2.10
PE 18:0/18:1	2.48
PE 18:0/18:0	1.6
PC 16:0/16:0	0.56
PC 16:0/18:1	0.68
PC 18:1/18:1	1.93
PC 18:0/18:1	0.67
PC 18:0/18:0	0.66
PC 20:0/20:0	0.55
PC 21:0/21:0	0.29

In order to determine the exact quantity of the unknown lipids calibration curves for each respective lipid would need to be created. While this is possible, it was determined that the advantages of exact quantitation did not outweigh the time and resources required to create the necessary calibration curves.

5.2 Syncrude Composite Tailings Well Water Samples and Multivariate Analysis

The method demonstrated in this thesis has shown that by using multivariate analysis it is possible to discern differences amongst the phospholipids present in the well water samples of the Syncrude composite tailings for the detectable phospholipids. The limit of detection achieved was approximately 13 nM for phosphatidylethanolamines and 22 nM for phosphatidylcholines as determined by the response of the calibration curve standards at the lowest concentration observed with respect to the noise of the instrument and using a definition of LOD as 3x signal to noise ratio.

As previously shown in section 3.3, the structure of the phospholipids can be obtained through the use of MS/MS spectroscopy. By using product ion scans the mass of each of the tail units can be determined. While this was observed to work effectively for standards as seen with PC 16:0/14:0, the results when examining the unknown PC at m/z 858 and PE at m/z 816 showed that when working with an unknown phospholipid the structure is significantly more difficult to discern with high confidence. For the chemical standards measured, the typical spectrum showed a fragment peak corresponding to the loss of the head unit as the most intense signal (100% abundance) with additional peaks corresponding to the loss of tail units between 8-

15% abundance. For the unknown phospholipid, the parent ion is the 100% abundance peak and the loss of the head unit produces a peak at 50% abundance. Based on the ratio of percent abundance for the loss of head group versus the loss of the tail units observed with standards, 100% and 8-15% respectively, the tail units for the unknown phospholipid should produce peaks at the 4-7.5% abundance range. Unfortunately this range of abundance for the signal would be undiscernible from the noise and identification of the tails would not be possible. Further work is required to improve the method used for the identification of the tail structures of the unknown phospholipids in the sample.

The multivariate analysis provides evidence for multiple hypotheses that may work in tandem or independently to affect the profiles of the bacterial phospholipids. The first hypothesis is that changes in well temperatures cause changes in the phospholipid profiles. It has been shown extensively in the literature that changes in temperature have a direct influence on the phospholipid profiles in various organisms[17,19,48]. This hypothesis is supported when analyzing the OPLS-DA and PCA data for a given well across multiple time points as well as samples taken in a given month across multiple well locations. The OPLS-DA plot for Well 6a (Figure 4.8) across the four time points that were sampled shows that there are differences in the phospholipid profiles when comparing the samples taken from Well 6a in July 2011, February 2012, May 2012, and August 2012. The hypothesis is that as the temperature of the well changes the phospholipid profile of the bacterial community changes. It is quite feasible that the variation seen by the OPLS-DA analysis is simply the variation of phospholipid profile utilized by bacteria at different temperatures to maintain homeostasis[48]. For this hypothesis to be true it would then be expected that the Sump Vault would show a similar shift in phospholipid profiles.

When observing the OPLS-DA plot for the Sump Vault (Figure 4.10) the data shows that there is a significant difference between three groups of data, the first group are the samples taken in July 2011, the second group are the samples taken in August 2012 and the third and final group are the samples taken in February 2012, May 2012, and October 2011. As previously stated this may be a temperature effect or may be due to other changes occurring. Furthermore, the results suggest a combined effect from multiple sources as it would initially be expected that July and August would have comparable phospholipid profiles. However, when looking at the well temperature data that is available from the sampling times it does not show significant difference in the well temperatures with the July 2011 sample being at 12.7°C, the October 2011 sample being at 10.2°C and the August 2012 sample being at 10.85°C. This weakens the hypothesis that temperature has a significant role to play in the phospholipid composition of the endogenous bacteria. The fact that July and August are also significantly different leads to the argument that an additional factor had a significant effect on the phospholipid composition.

Based on the depth of well 8c, its temperature should not vary significantly; as such for the hypothesis that temperature plays a major role in the phospholipid profiles to be true there should be very little variation in the profiles of well 8c. The OPLS-DA plot for the three time points of sampling done for Well 8c (figure 4.12), July 2011, May 2012, and August 2012, show differences in phospholipid profiles that appear to support the previous hypothesis. The temperatures of the well during sampling are available for the May 2012 and August 2012 samples; they are 29.7°C and 20.1°C respectively. Based on these temperature differences it is reasonable to expect to see a difference in phospholipid profiles which is in fact the exact result we see lending support to the hypothesis that temperature has an impact on the phospholipid

profiles of the well samples. As the temperature data for July 2011 is not available it is difficult to include the July 2011 data in an argument to support or refuting this hypothesis.

Looking at the multivariate data for samples taken during the same time period but from different locations provides another perspective, for this hypothesis to be true is would be expected that for samples taken during July 2011 period, differences between the shallower and typically cooler wells, well 6a and the sump vault, and the deeper and warmer wells, well 8c and well 5d, would be noticeable. The OPLS-DA plot for all samples taken during July 2011 appears to be randomly distributed regardless of location and shows a lack of any real differences between phospholipid profiles. As only one well temperature is available, the July 2011 sump vault sample, at a temperature of 12.7°C, it is difficult to draw any major conclusions. Despite a lack of temperature data, it is expect that the shallow samples, well 6a and sump vault, will have similar temperature and be based on the ground water temperature. As such it is expected that well 6a will have a very similar temperature to the sump vault. The deeper wells are theoretically unaffected by ground water as there should be minimal ground water movement within the composite tailings and as such are expected to be warmer due to bacterial activity. Since there is no difference in phospholipid profiles it tends to refute the hypothesis that temperature is the main factor of phospholipid profiles.

Finally, the OPLS-DA plot for all samples taken during May 2012 (Figure 4.16) shows a distinct difference in phospholipid profiles in the different wells. This is quite interesting since it was expected that if the shift in phospholipid profile was related to temperature that there would be a significant shift at the various depths during the colder months. However, well temperature data is available for the deeper well samples, well 5d and well 8c; their temperatures were 27.3°C and 29.7°C respectively. As the temperatures are not significantly different their

differences in phospholipid profile cannot be attributed to this slight difference. This further diminishes the hypothesis that the phospholipid profile changes are temperature dependant. As such a different factor must be affecting the phospholipid profiles and a second hypothesis developed.

The second hypothesis for the cause of the differences in phospholipid profiles observed is that the changes made by Syncrude to the surface foliage of the fen had an impact on the bacterial communities. This may be through a change in nutrients available or through changes to the local environment including physical or chemical changes such as variations in pH or other factors. These changes may manifest as a shift in phospholipid profiles of the original bacterial community or shifts in the distribution of bacterial species within the community. Furthermore these changes to the bacterial community may be due to the changes made by Syncrude or could simply be independent and simply be a manifestation of the evolution of the composite tailings. If the shift in phospholipid profiles is due to changes to the surface of the fen made by Syncrude over the course of the one year period it would be expected that there would be a shift in phospholipid profiles as time passes. It is then expected that the phospholipid profiles will change over the course of the year for each individual well.

When observing the OPLS-DA data for well 6a (figure 4.8) it is obvious that there is a change in phospholipid profiles as time progresses. This is directly supporting the hypothesis that the change is associated with the evolution of the fen over the course of the year. For this hypothesis to hold true the same shift in profiles must be seen in the sump vault. The OPLS-DA data for the sump vault (figure 4.10) confirms that a shift in phospholipid profiles does occur over the course of the year. The fact that the cooler months of October 2011, February 2012, and May 2012 group together could be due to limited growth of the surface foliage or could be

independent and caused by a separate factor. Furthermore, there is also a shift in the phospholipid profile in well 8c over the course of the one year period as seen in the OPLS-DA plot (figure 4.12) adding further evidence for the change in the phospholipid profile as a result of the changes occurring over the course of the year from July 2011 to August 2012. If this were the only cause of the changes in the phospholipid profile it would then be expected that there would be no differences in phospholipid profiles for wells that were sampled at the same time. This is not the case, when looking at the OPLS-DA plot for May 2012 (figure 4.16), there are clear differences in the phospholipid profiles that must be caused by a factor other than the passing of time.

Further studies, outside the scope of this thesis, would be required to identify whether these changes in phospholipid profiles are due to the changing foliage of the Syncrude Sandhill Fen or simply a shift in the bacterial community due other factors. Furthermore, it is clear that there is more than one factor effecting the change of the phospholipid profiles and that it is more complex that any individual hypothesis presented here.

5.3 Syncrude Composite Tailings Well Sediment Samples

Using the modified Blight and Dyer method for the analysis of the sediment samples from the Syncrude composite tailings site was unsuccessful due to excessive ion suppression and poor extraction recoveries. The evidence for this is easily seen in figure 4.21; the lack of a signal for the recovery standards could be caused by one of two things. The first is due to poor chemical recovery during the extraction process although since the extraction process is similar to that

used for the water samples it is difficult to assume that this is the issue. The following cleanup steps are unique to the sediment samples and as such could be the cause of the poor recoveries. The silica column setup used for this analysis has been shown to work by the Dr. Slater group[49], as such the other possibility is that the silica column has not removed enough of the contaminants present for the analysis of phospholipids by direct-infusion. This is the cause of the ion suppression that is seen and significantly limits the instruments ability to quantitatively detect all ions as they enter the instrument and as such certain ions would no longer be registered by the detector and results in approximately a one order of magnitude reduction in the signal intensities of the internal standards.

This issue of ion suppression would only be solved through the use of separation by LC or additional sample preparation. As such after a significant amount of optimization it was determined that direct-infusion lipidomics is not a suitable method for the analysis of phospholipids in sediment samples containing a significant amount of organic material.

Chapter 6: Conclusion and Future Direction

6.1 Conclusions

The main goal of this thesis centered on the modification and optimization of a previously developed direct-infusion mass spectrometry method for the analysis of phospholipids in unknown samples. To date the majority of phospholipid work has centered around the analysis of concentrated bacteria cultures, whereas this thesis aimed to develop methodogy to analyze water and sediment samples containing low concentrations of phospholipids and high concentrations of other organic contaminants.

This thesis began with the optimization of the previous method for the analysis of water samples collected from the Syncrude Sandhill composite tailing fen. The instrument parameters were optimized to provide the best possible detection limits and the extraction method modified to be used with water samples containing an inherently low concentration of phospholipids (chapter 3). The optimization was meant to deal with the issue of low phospholipid concentrations and reduce the impact on the spectrum by contaminants. While this was successful for use in water samples, it was unfortunately unable to handle the amount of organic material, including left over bitumen and other petroleum products, found in the sediment samples. The other aspect of optimization of the procedure was the development of a method for the identification of the phospholipids based on exact mass. Since a public database of all possible phospholipids is not available, one was created to include the monoisotopic masses of Li^+ adducts. The second database required was for the identification of phospholipid tail

structures based on fragmentation patterns, again a database was created containing the unique Li^+ adducts of all potential tail fragmentations.

Upon optimization of the analytical methodology, both Syncrude composite tailings well water samples and sediment samples were analyzed and multivariate statistical analysis were performed. This thesis revealed trends within the phospholipid profiles both within an individual well across a one year time period and also all well samples across time. It was hypothesized that the changes occurring over time both through the natural changes in the composite tailing as well as the changes introduced by Syncrude would have the greatest impact on the phospholipid profile and that the well temperature would have a smaller but still significant impact on the profile. Further work is needed to compare the phospholipid profiles obtained with those of specific bacterial classes with respect to determining shifts within the bacterial community and is discussed in the future directions.

6.2 Future Directions

The work presented in this thesis provided a glimpse into the trends present in the phospholipid profiles across a one year period within the composite tailings fen. There are several directions for this work to continue.

One possibility is the further development of the extraction method for the sediment samples. This would improve the understanding of the changes in the phospholipid profiles at the surface of the fen and may help to elucidate the changes occurring at depth. This would almost certainly require separation prior to mass spectrometry through the use of high performance liquid chromatography (HPLC) to alleviate ion suppression due to the large quantities of organic material present in these samples. In addition to the reduction of ion suppression, the development of an HPLC-MS method would also impart a number of other analytical advantages. Since each phospholipid would elute in a defined retention range the use of individual MRM transitions may be used which should have a positive impact on sensitivity thereby lowering the detection limits compared to using product ion scans. Utilizing retention time data will also aid in identification of phospholipids beyond what tandem MS can provide.

Finally, an additional future direction which may be taken as a result of the work presented in this thesis is a more rigorous study of tailing ponds and wells may be started including the close monitoring of ambient conditions such as water and air temperature. The hypotheses generated in this work suggest that temperature has an impact on the phospholipid profile found in well water and likely sediment. Knowing the temperature trends found in these environments to an accurate degree may aid in predicting how effectively the natural

biota can remediate any water/sediment contamination in the future. Also, this additional work would allow for the phospholipid profiles to be compared with those of sulphate reducing bacteria as well as other bacterial classes to tie back into the project goal of monitoring bacterial community changes.

References

(1) Syncrude Canada Ltd Oil Sands History http://www.syncrude.ca/users/folder.asp?FolderID=5657 (accessed Aug 27, 2013).

(2) Abraham, H. *Asphalts and Allied Substances*; D. Van Nostrand Company Inc, 1938.

(3) Alberta Onlina Encyclopedia Karl Clark http://wayback.archive-it.org/2217/20101208161839/http://www.edukits.ca/petroleum/focus_people_clark.htm (accessed Aug 28, 2013).

(4) Comfort, D. J. *The Abasand Fiasco*; Friesen Printers: Edmonton, 1980.

(5) Syncrude Canada Ltd About Syncrude http://www.syncrude.ca/users/folder.asp?FolderID=5617 (accessed Aug 27, 2013).

(6) Oil & Gas Journal **2012**, *110*, 15–17.

(7) Gu, G.; Xu, Z.; Nandakumar, K.; Masliyah, J. H. **1938**, *81*, 1859–1869.

(8) Matthews, J.; Shaw, W. *International Journal of …* **2002**, 37–41.

(9) Canadian Petroleum Hall of Fame Dr. Roger M. Butler http://www.canadianpetroleumhalloffame.ca/roger-butler.html (accessed Aug 28, 2013).

(10) Deutsch, C. V; Mclennan, J. A. *Centre for Computational Geostatistics* **2005**, *3*.

(11) Ratledge, C.; Wilkinson, S. G. *Microbial Lipids Volume 1*; Academic Press: London, 1988.

(12) Harwood, J. L.; Russell, N. J. *Lipids in Plants and Microbes*; George Allen and Unwin: London, 1984.

(13) Lodish, H. F. *Molecular cell biology*; W. H. Freeman: New York, 2000; p. 1084.

(14) Spector, a a; Yorek, M. a *Journal of lipid research* **1985**, *26*, 1015–35.

(15) Kaduce, T.; Awad, A. *Journal of Biological …* **1977**, *252*, 6624–30.

(16) Szamel, M.; Resch, K. *Journal of Biological Chemistry* **1981**, *256*, 11618–11623.

(17) Murata, N.; Los, D. *Plant Physiology* **1997**, *115*, 875–879.

(18) Sato, N.; Murata, N. *Biochimica et Biophysica Acta* **1980**, *619*, 353–366.

(19) Petersen, S. O.; Klug, M. J.; Petersen, S.; Klug, M. J. *APPL. ENVIRON. MICROBIOL* **1994**, *60*.

(20) Patti, G. J.; Yanes, O.; Siuzdak, G. *Nature reviews. Molecular cell biology* **2012**, *13*, 263–9.

(21) Oliver, S.; Winson, M.; Kell, D.; Baganz, F. *Trends in biotechnology* **1998**, *16*, 373–378.

(22) Han, X.; Gross, R. W. *Journal of lipid research* **2003**, *44*, 1071–9.

(23) Han, X.; Gross, R. W. *Mass spectrometry reviews* **2005**, *24*, 367–412.

(24) Basconcillo, L. S.; Zaheer, R.; Finan, T. M.; McCarry, B. E. *Journal of lipid research* **2009**, *50*, 1120–32.

(25) Basconcillo, L. S.; Zaheer, R.; Finan, T. M.; McCarry, B. E. *Journal of chromatography. B, Analytical technologies in the biomedical and life sciences* **2009**, *877*, 2873–82.

(26) Han, X.; Yang, K. *Mass Spectrometry Reviews* **2012**, 134–178.

(27) Chalcraft, K. R.; McCarry, B. E. Comprehensive Metabolomics of Peanut Allergy, McMaster University, 2013.

(28) Basconcillo, L. S.; McCarry, B. E. *Journal of chromatography. B, Analytical technologies in the biomedical and life sciences* **2008**, *871*, 22–31.

(29) Zelles, L. *Biology and Fertility of Soils* **1999**, 111–129.

(30) Harwood, J. *Gas chromatography and lipids: A practical guide:*; 1989; Vol. 28, pp. 3251–3252.

(31) Cowie, B. R.; Slater, G. F.; Bernier, L.; Warren, L. a. *Organic Geochemistry* **2009**, *40*, 956–962.

(32) Lee, S. H.; Blair, I. a *BMB reports* **2009**, *42*, 401–10.

(33) Imbert, L.; Gaudin, M.; Libong, D.; Touboul, D.; Abreu, S.; Loiseau, P. M.; Laprévote, O.; Chaminade, P. *Journal of chromatography. A* **2012**, *1242*, 75–83.

(34) Veloso, A.; Fernández, R.; Astigarraga, E.; Barreda-Gómez, G.; Manuel, I.; Giralt, M. T.; Ferrer, I.; Ochoa, B.; Rodríguez-Puertas, R.; Fernández, J. a *Analytical and bioanalytical chemistry* **2011**, *401*, 89–101.

(35) Fernández, J. a; Ochoa, B.; Fresnedo, O.; Giralt, M. T.; Rodríguez-Puertas, R. *Analytical and bioanalytical chemistry* **2011**, *401*, 29–51.

(36) Van der Werf, I. D.; Calvano, C. D.; Palmisano, F.; Sabbatini, L. *Analytica chimica acta* **2012**, *718*, 1–10.

(37) Knochenmuss, R. *The Analyst* **2006**, *131*, 966–86.

(38) Chapman, S. *Phys. Rev. Lett.* **1937**, *52*, 184–190.

(39) Iribarne, J.; Thomson, B. *The Journal of Chemical Physics* **1976**.

(40) Dole, M.; Mack, L.; Hines, R. *The Journal of …* **1968**.

(41) Chalcraft, K. R.; Lee, R.; Mills, C.; Britz-mckibbin, P. *Anal Chem* **2009**, *81*, 2506–2515.

(42) Annesley, T. M. *Clinical chemistry* **2003**, *49*, 1041–4.

(43) Warren, L. a. Sampling Methods **2012**.

(44) Bligh, E. *Canadian journal of biochemistry and* **1959**, *505*, 1 5.

(45) Basconcillo, L. S.; Zaheer, R.; Finan, T. M.; McCarry, B. E. *Microbiology (Reading, England)* **2009**, *155*, 373–85.

(46) Voyksner, R. D. Advantages of Orthogonal Nebulizer Orientation in Electrospray for Quadrupole and Ion Trap Mass Spectrometers Technical Note **2001**, 1–7.

(47) Basconcillo, L. S.; McCarry, B. E. No Title, McMaster University, 2009.

(48) Hazel, J. R. *The American journal of physiology* **1984**, *246*, R460–70.

(49) Ngonadi, N.; Slater, G. F. Using PLFA to constrain microbial distribution related to S-cycling in oil-sands composite tailings during reclamation, McMaster, 2013.

(50) Canadian Association of Petroleum Producers **2013**.

Appendix 1: List of Chemical Standards Used

Name	Abbreviation	Molar mass
1,2-didecanoyl-sn-glycero-3-phosphate	PA 10:0/10:0	502.267
1,2-dilauroyl-sn-glycero-3-phosphate	PA 12:0/12:0	558.330
1,2-dipalmitoyl-sn-glycero-3-phosphate	PA 16:0/16:0	670.455
1-palmitoyl-2-oleoyl-sn-glycero-3-phosphate	PA 16:0/18:1	696.471
1,2-dilinoleoyl-sn-glycero-3-phosphate	PA 18:2/18:2	718.455
1,2-dioleoyl-sn-glycero-3-phosphate	PA 18:1/18:1	722.486
1,2-distearoyl-sn-glycero-3-phosphate	PA 18:0/18:0	726.518
1,2-dilauroyl-sn-glycero-3-phospho-(1'-rac-glycerol)	PG 12:0/12:0	632.367
1,2-dipalmitoyl-sn-glycero-3-phospho-(1'-rac-glycerol)	PG 16:0/16:0	744.492
1,2-diheptadecanoyl-sn-glycero-3-phospho-(1'-rac-glycerol)	PG 17:0/17:0	772.523
1,2-dilinoleoyl-sn-glycero-3-phospho-(1'-rac-glycerol)	PG 18:2/18:2	792.492
1,2-dioleoyl-sn-glycero-3-phospho-(1'-rac-glycerol)	PG 18:1/18:1	796.523

1-stearoyl-2-oleoyl-sn-glycero-3-phospho-(1'-rac-glycerol)	PG 18:0/18:1	798.539
1,2-distearoyl-sn-glycero-3-phospho-(1'-rac-glycerol)	PG 18:0/18:0	800.554
1,2-didecanoyl-sn-glycero-3-phospho-L-serine	PS 10:0/10:0	589.299
1,2-dimyristoyl-sn-glycero-3-phospho-L-serine	PS 14:0/14:0	701.424
1,2-dioleoyl-sn-glycero-3-phospho-L-serine	PS 18:1/18:1	809.518
1,2-distearoyl-sn-glycero-3-phospho-L-serine	PS 18:0/18:0	813.550
1,2-dilauroyl-sn-glycero-3-phosphocholine	PC 12:0/12:0	621.826
1-myristoyl-2-palmitoyl-sn-glycero-3-phosphocholine	PC 14:0/16:0	705.531
1,2-dipalmitoyl-sn-glycero-3-phosphocholine	PC 16:0/16:0	733.562
1-palmitoyl-2-oleoyl-sn-glycero-3-phosphocholine	PC 16:0/18:1	759.578
1,2-dilinoleoyl-sn-glycero-3-phosphocholine	PC 18:2/18:2	781.562
1,2-dioleoyl-sn-glycero-3-phosphocholine	PC 18:1/18:1	785.593
1-stearoyl-2-oleoyl-sn-glycero-3-phosphocholine	PC 18:0/18:1	787.609

1,2-distearoyl-sn-glycero-3-phosphocholine	PC 18:0/18:0	789.625
1,2-diarachidoyl-sn-glycero-3-phosphocholine	PC 20:0/20:0	845.687
1,2-dihenarachidoyl-sn-glycero-3-phosphocholine	PC 21:0/21:0	873.719
1,2-dioctanoyl-sn-glycero-3-phosphoethanolamine	PE 8:0/8:0	467.265
1,2-dilauroyl-sn-glycero-3-phosphoethanolamine	PE 12:0/12:0	579.390
1,2-dimyristoyl-sn-glycero-3-phosphoethanolamine	PE 14:0/14:0	635.453
1,2-dipalmitoyl-sn-glycero-3-phosphoethanolamine	PE 16:0/16:0	691.515
1,2-dioleoyl-sn-glycero-3-phosphoethanolamine	PE 18:1/18:1	743.547
1-stearoyl-2-oleoyl-sn-glycero-3-phosphoethanolamine	PE 18:0/18:1	745.562
1,2-distearoyl-sn-glycero-3-phosphoethanolamine	PE 18:0/18:0	747.578